

# Fitting multivariate Hawkes processes to interval count data with an application to terrorist activity modelling – a particle Markov chain Monte Carlo approach

Jason J. Lambe<sup>1, 2, 3</sup>, Feng Chen<sup>1</sup>, Tom Stindl<sup>1</sup>, and Tsz-Kit Jeffrey Kwan<sup>1</sup>

<sup>1</sup>UNSW School of Mathematics and Statistics, Sydney, Australia

<sup>2</sup>Defence Science and Technology Group, Sydney, Australia

<sup>3</sup>Corresponding Author

March 25, 2025

## Abstract

Terrorist activities often exhibit temporal and spatial clustering, making the multivariate Hawkes process (MHP) a useful statistical model for analysing terrorism across different geographic regions. However, terror attack data from the Global Terrorism Database is reported as total event counts in disjoint observation periods, with precise event times unknown. When the MHP is only observed discretely, the likelihood function becomes intractable, hindering likelihood-based inference. To address this, we design an unbiased estimate of the intractable likelihood function using sequential Monte Carlo (SMC) based on a representation of the unobserved event times as latent variables in a state-space model. The unbiasedness of the SMC estimate allows for its use in place of the true likelihood in a Metropolis-Hastings algorithm, from which we construct a Markov Chain Monte Carlo sample of the distribution over the parameters of the MHP. Using simulated data, we assess the performance of our method and

demonstrate that it outperforms an alternative method in the literature based on mean squared error. Terrorist activity in Afghanistan and Pakistan from 2018 to 2021 is analysed based on daily count data to examine the self- and cross-excitation effects of terrorism events.

## 1 Introduction

Terrorism, defined for the *Global Terrorism Database* (GTD, 2022) as “the threatened or actual use of illegal force and violence by a non-state actor to attain a political, economic, religious, or social goal through fear, coercion, or intimidation” is a widespread issue, with terrorist events having occurred in an average of 95 nations annually from 2010 to 2020 (GTD, 2022). Understanding the patterns of terrorist activity aids in the evaluation of terrorism counter-measures; a topic which has long been of interest to criminology researchers (Midlarsky et al., 1980; Behlendorf et al., 2012; Rieber-Mohn and Tripathi, 2021) and policy makers alike (Perl, 2007; White et al., 2014).

Terrorist attacks are known to exhibit spatiotemporal clustering. For instance, Midlarsky et al. (1980) found that the spread of international terrorism in Latin America and Western Europe in the period 1968-1974 exhibited *contagion* effects. More recently, Behlendorf et al. (2012) found evidence that terrorist attacks carried out, respectively, by organisations FMLN in El Salvador and ETA in Spain displayed similar spatiotemporal clustering behaviour, despite differences in history and motive of the two groups. Localised bursts of terrorist activity were also identified in relation to the Taliban insurgency in Afghanistan in 2016 (Rieber-Mohn and Tripathi, 2021).

The Hawkes process (Hawkes, 1971) is a *self-exciting* point process, meaning that the occurrence of an event causes a short-term spike in the arrival rate of subsequent events. The multivariate Hawkes process (MHP) is a multidimensional extension of the Hawkes process in which events of finitely many *types* can both self-excite events of the same type and *cross-excite* events of other types. Given the apparent clustering behaviour of political violence, the MHP is an appropriate model for terrorist activity across multiple groups or regions (Tench et al., 2016; Zhou and Papadogeorgou, 2023; Jun and Cook, 2024). More broadly, the MHP is useful in application domains where excitation is seen across multiple processes, such as joint analysis of activity in a neuron cluster (Bonnet et al., 2022), financial market transactions during periods of positive or negative returns and market sentiment

(Yang et al., 2018), and the spread of infectious disease between cities or nations (Chen et al., 2022).

The Maximum Likelihood Estimator (MLE) can be calculated for both the Hawkes process (Ogata, 1978) and the MHP (Bowsher, 2007). Expectation Maximisation (EM) algorithms are also commonly used to estimate the MHP as they can mitigate the instability that may arise when numerically maximising the log-likelihood surface, which is often flat or multimodal (Veen and Schoenberg, 2008). However, both the MLE and the EM methods require knowledge of the precise event times over the span of observation. There are a variety of reasons that event time data may be aggregated for relevant applications of the MHP, such as the imprecise reporting of terror attacks (Tench et al., 2016), the inability of an affected individual to identify the time they became infected by a disease (Chen et al., 2022), or where finite measurement precision makes it appear that financial transactions have occurred simultaneously (Bowsher, 2007). When a point process is only observed discretely, the likelihood function is analytically intractable, which poses a challenge for conducting inference on the MHP.

Prior applications of the Hawkes process to terrorism have employed various techniques to handle aggregated data. Porter and White (2012) use a *hurdle* model of the type described in Mullahy (1986) when working with daily attack counts from Indonesia (1994 - 2007). A Bernoulli process, specified using a discretised version of the Hawkes intensity process, determines whether any events occur on a given day, with the number of events subsequently chosen from a probability mass function. Discretising the Hawkes process only allows Porter and White (2012) to model excitation effects to the accuracy of a single observation window. Tench et al. (2016) use a MHP to model improvised explosive device (IED) attacks across counties in Northern Ireland (1970 - 1998), with data aggregated daily. In the case where an individual county or city has multiple events per day, they simply count this as one event, inducing some information loss. Though there were rarely multiple terror events on a single day in Northern Ireland over this time period, this approach is clearly not scalable to settings with heavier aggregation. When events of different types occur on the same day, Tench et al. (2016) randomly perturb the event times according to the method of Bowsher (2007). Perturbation of location coordinates is used by Jun and Cook (2024) in their spatiotemporal Hawkes process model of terrorism in Afghanistan when multiple events at a given location occur in the same observation window.

Recent works have presented methods for fitting the MHP with aggre-

gated data. An early method is given by [Kirchner \(2017\)](#), which approximates the likelihood of the discretely observed MHP by a sequence of order  $p$  Integer-Valued Autoregressions (INAR), from which an estimator is obtained. This method is justified by a weak convergence of a sequence of INAR( $\infty$ ) models to the MHP as the width of the observation intervals approaches zero. [Shlomovich et al. \(2022a\)](#) use a modified Monte Carlo Expectation Maximisation (MCEM) algorithm to estimate the MHP with discretely observed data, with flexibility to handle differently sized observation periods. In the E-step of the algorithm, the authors sequentially reconstruct the latent event times by selecting the mode of a proposal distribution truncated over each observation period. This differs from typical MCEM methods as the hidden times are chosen deterministically instead of randomly sampled. The MCEM estimators appear to be biased in general, though simulation experiments in [Shlomovich et al. \(2022a\)](#) demonstrate the superiority of this method over the INAR( $p$ ) approach of [Kirchner \(2017\)](#). The estimation of standard errors of the MCEM estimates is not addressed in [Shlomovich et al. \(2022a\)](#).

Other methods are available in the univariate case. A quasi-likelihood approach is taken by [Rizoiu et al. \(2022\)](#), whereby the observed count data is assumed to be generated by an inhomogeneous Poisson process with intensity given by the mean intensity process of the Hawkes process. The MLE is then calculated directly. [Calderon et al. \(2023\)](#) extend this work to the MHP where a subset of the dimensions are discretely observed, with the remainder continuously observed. Their method is not applicable to the stationary Hawkes process as the mean intensity process is constant, rendering the parameters unidentifiable. [Cheysson and Lang \(2022\)](#) obtain a consistent and asymptotically normal estimator from the spectral density of the stationary Hawkes process, though they rely on the assumption that the aggregation windows are of equal length. The synthetic method of [Schneider and Weber \(2023\)](#) involves simulating a sample path, manually altering it via thinning (removing events) or thickening (adding events) such that it agrees with the observed count data, updating the estimate via EM or MLE, and repeating until convergence. Simulation experiments in [Schneider and Weber \(2023\)](#) show comparable performance to the MCEM estimator ([Shlomovich et al., 2022b](#)), and the computation of standard error estimates is also not addressed.

When the likelihood function can be evaluated exactly, one can use Markov Chain Monte Carlo (MCMC) to approximate the MLE. Using an improper uniform prior on the parameter, the posterior is proportional to the likelihood

function, from which a sample is drawn via MCMC. It is well established that when a parametric model satisfies certain differentiability conditions, the posterior over the parameter space converges to a Gaussian distribution (van der Vaart, 1998). Hence, the MLE can then be approximated as the median of the resulting MCMC chain.

Motivated by the challenges of modelling terrorist activity using the discretely observed MHP, in this work, we propose to obtain an unbiased estimator of the likelihood function via *sequential Monte Carlo* (SMC) by extending the methods in Chen et al. (2025). The SMC estimate is then used in place of the true likelihood in an otherwise typical Metropolis-Hastings algorithm (Metropolis et al., 1953; Hastings, 1970), commonly known as the Pseudo-Marginal Metropolis-Hastings (PMMH; Andrieu and Roberts, 2009) algorithm, which yields the true likelihood distribution (or more generally, the posterior distribution) as the stationary distribution of the resulting MCMC sample, from which the estimates are computed.

Our proposed methodology solves the multivariate estimation problem with significantly less empirical bias than the MCEM technique, which to date is the lone competitor in the multivariate setting. The SMC likelihood estimation method is flexible to handle discrete data with observation windows of unequal length, and the PMMH procedure allows for a simple calculation of standard error estimates. These are both advantages over MCEM. Where Chen et al. (2025) use a Poisson process to propose event times in their implementation of the SMC procedure, we instead use an ordered uniform distribution over each observation window. This choice improves efficiency by guaranteeing that all proposals agree with the observed data. Numerical experiments demonstrate that in the multivariate setting, using uniform proposals in place of Poisson proposals dramatically reduces the variance of the SMC estimates, which is crucial for ensuring the efficiency of the PMMH algorithm without requiring prohibitively large numbers of particles. In application to discretely observed terror attack data, our estimation procedure enables the MHP to be fit directly without requiring the data augmentation or model discretisation techniques that have historically been used.

The article is organised as follows. In Section 2, we introduce the MHP model, formally set up the estimation problem, and present the estimation method. Simulation studies are performed in Section 3. The uniform proposal distribution is numerically compared to the Poisson proposals, and the performance of the PMMH algorithm is assessed using simulated data with varied levels of aggregation. The resulting estimates are compared to the

MCEM estimators of [Shlomovich et al. \(2022a\)](#). In Section 4, the proposed method is used to estimate a bivariate Hawkes process model of terrorist activity in Afghanistan and Pakistan. The article concludes with a short discussion in Section 5. Detailed derivations and additional figures can be found in the appendices.

## 2 Data, Model and Estimation Method

Let  $\{(\tau_i, z_i)\}_{i \in \mathbb{N}}$  denote a realisation of a multivariate point process. The sequence  $\{\tau_i\}_{i \in \mathbb{N}}$  is assumed to be strictly positive and strictly increasing, with the value  $\tau_i$  interpreted as the  $i^{\text{th}}$  event time after an initial time  $t = 0$ . For some  $M \in \mathbb{N}$ , the value  $z_i \in \{1, \dots, M\} =: \mathcal{M}$  represents the *type* of the  $i^{\text{th}}$  event. This structure gives rise to the  $M$ -dimensional counting process

$$\mathbf{N}_t = (N_1(t), \dots, N_M(t)),$$

with  $N_m(t)$  being the number of type- $m$  events to time  $t$ . More generally,  $N_m(A)$  is the number of events on a set  $A \in \mathcal{B}(\mathbb{R}_+)$ . The history of the process is represented by the filtration  $\{\mathcal{F}_t\}_{t \geq 0}$ , with  $\mathcal{F}_t = \sigma\{\mathbf{N}_s : s \leq t\}$ . To specify the model as an MHP, we use the conditional intensity vector  $\boldsymbol{\lambda} : \mathbb{R}_+ \rightarrow \mathbb{R}_+^M$ , with  $m^{\text{th}}$  component  $\lambda_m : \mathbb{R}_+ \rightarrow \mathbb{R}_+$  defined as

$$\begin{aligned} \lambda_m(t) &:= \frac{\mathbb{E}[\mathrm{d}N_m(t) | \mathcal{F}_{t-}]}{\mathrm{d}t} = \nu_m(t) + \sum_{k: \tau_k < t} \eta_{m, z_k} h_{m, z_k}(t - \tau_k) \\ &=: \nu_m(t) + \varphi_m(t), \end{aligned}$$

where  $\mathcal{F}_{t-} = \sigma\{\mathbf{N}_s : s < t\}$ . The function  $\nu_m : \mathbb{R}_+ \rightarrow \mathbb{R}_+$  determines the background arrival rate for type- $m$  events. The *excitation kernel* functions  $h_{m,j}(\cdot)$ ,  $m, j \in \mathcal{M}$ , are probability density functions having support  $\mathbb{R}_+$ , which control the shape of the excitation effect of type- $j$  events on type- $m$  event intensity. They are also referred to as the *offspring density functions* due to the cluster Poisson process interpretation of Hawkes processes ([Hawkes and Oakes, 1974](#)). The offspring density function determines the birth time distribution of generation-1 offspring events of type- $m$  due to a type- $j$  event, given at least one such event. The *branching ratios*  $\eta_{m,j}$ ,  $m, j \in \mathcal{M}$ , are positive constants that represent the respective expected numbers of generation-1 offspring events of type- $m$  due to a type- $j$  event.

Together,  $\eta_{m,j} h_{m,j}(\cdot)$  is called the *excitation function*, henceforth written as  $g_{m,j}(\cdot)$ . Let  $\eta = (\eta_{mj})_{m,j \in \mathcal{M}}$  be the matrix of branching ratios. To ensure the stability of the model, it is assumed that  $\rho(\eta) < 1$ , with  $\rho(A)$  denoting the spectral radius, or the maximum absolute value of the eigenvalues, of the matrix  $A$ . With this stability condition, in the case where all background rate functions  $\nu_m(\cdot)$  satisfy  $\nu_m(t) = \nu_m \in \mathbb{R}_+$ , the mean arrival rates of events of different types approach finite values given by

$$\lim_{t \rightarrow \infty} \mathbb{E}([\lambda_1(t), \dots, \lambda_M(t)]^\top) = (\mathcal{I} - \eta)^{-1}(\nu_1, \dots, \nu_M)^\top,$$

with  $\mathcal{I}$  denoting the  $M \times M$  identity matrix. It is further assumed that  $h_{m,j}$  depends on a vector of parameters,  $\theta_{m,j}$ , with the vector of all parameters (including values of  $\nu_m$  and  $\eta_{m,j}$ ) labelled as  $\theta$ .

The MHP induces the *total process*  $N^*$ , defined by  $N^*(t) = \sum_{m=1}^M N_m(t)$ , which counts events of all types to time  $t$ . The intensity process of  $N^*$ , referred to as the *total intensity*, is given by

$$\lambda^*(t) = \sum_{m=1}^M \lambda_m(t) = \nu(t) + \sum_{m=1}^M \varphi_m(t)$$

where we write  $\nu(t) := \sum_m \nu_m(t)$  as the total background arrival rate. The notation  $N_i^* = N^*(t_i)$  will be used throughout.

## 2.1 Data and Likelihood

The log-likelihood for a MHP observed on interval  $(0, T]$ , when the precise event times are known, has the form

$$\log L_c(\theta) = \sum_{k: \tau_k < T} \log \lambda_{z_k}(\tau_k) + \int_0^T \lambda^*(t) dt,$$

see for example [Daley and Vere-Jones \(2003\)](#). However, when only aggregated data is observed for each event type at fixed time points, we must resort to an approximation of the likelihood. Let there be  $I \in \mathbb{Z}_+$  observation times, satisfying  $0 = t_0 < t_1 < \dots < t_I = T$ . At each time  $t_i$ , the vector

$$\mathbf{n}_i = (n_{i,1}, \dots, n_{i,M})$$

is observed, where  $n_{i,m}$  represents the realised value of  $N_m(t_{i-1}, t_i]$ . The likelihood function is then given by

$$L(\theta) = P_\theta(N_m(t_{i-1}, t_i] = n_{i,m}, m \in \mathcal{M}, i = 1, \dots, I).$$

For notational convenience, we write  $P_\theta(N_m(t_{i-1}, t_i] = n_{i,m})$  as  $p(n_{i,m})$ , with dependence on  $\theta$  being implicitly understood. We will also use the colon notation for a collection of indexed variables or values, such that  $x_{k:l} = (x_k, \dots, x_l)$  for  $k < l$ .

## 2.2 Sequential Monte Carlo estimation of the likelihood

The sequence of *filtering* distributions  $P(d(\tau, z)_{1:N_i^*} | \mathbf{n}_{1:i})$  are sampled from using SMC, with a sample at time  $t_i$  obtained from the existing sample at time  $t_{i-1}$  via a two-step Bayesian updating procedure. An unbiased estimate of the likelihood function is then derived using the factorisation

$$\begin{aligned} L(\theta) &= \prod_{i=1}^I p(\mathbf{n}_i | \mathbf{n}_{1:i-1}) \\ &= \prod_{i=1}^I \int p(\mathbf{n}_i | (\tau, z)_{1:N_i^*}, \mathbf{n}_{1:i-1}) P(d(\tau, z)_{1:N_{i-1}^*} | \mathbf{n}_{1:i-1}) \\ &\quad \times P(d(\tau, z)_{N_{i-1}^*+1:N_i^*} | (\tau, z)_{1:N_{i-1}^*}, \mathbf{n}_{1:i-1}). \end{aligned} \quad (1)$$

To obtain the initial sample, the filtering distribution at time  $t_1$  is first written as

$$P(d(\tau, z)_{1:N_1^*}, | \mathbf{n}_1) \propto p(\mathbf{n}_1 | (\tau, z)_{1:N_1^*}) P(d(\tau, z)_{1:N_1^*}).$$

This is akin to the representation of a posterior, here being the filtering distribution, as proportional to the prior (predictive distribution) combined with a likelihood factor (Pitt and Shephard, 1999). A collection of  $J$  *particles*, written as  $(\tau, z)_{1:N_1^*}^{(1:J)}$ , are sampled from a proposal distribution  $Q(d(\tau, z)_{1:N_1^*} | \mathbf{n}_1)$ . Note that the proposal distribution is allowed to depend on  $\mathbf{n}_1$ . This approach, sometimes termed the *guided particle filter*, ensures that the proposals agree with the observation, and requires only that the proposal distribution dominates the filtering distribution (Chopin and Papaspiliopoulos,

2020). Each particle has an associated importance weight

$$w_1^{(j)} = \frac{p(\mathbf{n}_1 \mid (\tau, z)_{1:N_1^*}) P(d(\tau, z)_{1:N_1^*})}{Q(d(\tau, z)_{1:N_1^*} \mid \mathbf{n}_1)} \Big|_{(\tau, z)_{1:N_1^*} = (\tau, z)_{1:N_1^*}^{(j)}}.$$

Let  $W_1^{(j)}$  denote the  $j^{\text{th}}$  normalised weight. From (1), the SMC estimates of the filtering distribution and marginal likelihood factor,  $p(\mathbf{n}_1)$ , are given respectively by

$$\begin{aligned} \widehat{P}(d(\tau, z)_{1:N_1^*} \mid \mathbf{n}_1) &= \sum_{j=1}^J W_1^{(j)} \delta_{(\tau, z)_{1:N_1^*}^{(j)}}(d(\tau, z)_{1:N_1^*}), \\ \hat{p}(\mathbf{n}_1) &= \frac{1}{J} \sum_{j=1}^J w_1^{(j)}. \end{aligned}$$

Suppose that at time  $t_{i-1}$  we have a sample  $(\tau, z)_{1:N_{i-1}^*}^{(1:J)}$  from the filtering distribution, with associated estimate  $\widehat{P}(d(\tau, z)_{1:N_{i-1}^*} \mid \mathbf{n}_{1:i-1})$ . The filtering distribution at time  $t_i$  is given by

$$\begin{aligned} &P(d(\tau, z)_{1:N_i^*} \mid \mathbf{n}_{1:i}) \\ &\propto p(\mathbf{n}_i \mid (\tau, z)_{1:N_i^*}, \mathbf{n}_{1:i-1}) P(d(\tau, z)_{1:N_i^*} \mid \mathbf{n}_{1:i-1}) \\ &= p(\mathbf{n}_i \mid (\tau, z)_{1:N_i^*}, \mathbf{n}_{1:i-1}) P(d(\tau, z)_{N_{i-1}^*+1:N_i^*} \mid (\tau, z)_{1:N_{i-1}^*}, \mathbf{n}_{1:i-1}) \\ &\quad \times P(d(\tau, z)_{1:N_{i-1}^*} \mid \mathbf{n}_{1:i-1}). \end{aligned}$$

This representation motivates the following sequential sampling procedure. We first generate a sample

$$(\tilde{\tau}, \tilde{z})_{1:N_{i-1}^*}^{(1:J)} \stackrel{\text{iid}}{\sim} \widehat{P}(d(\tau, z)_{1:N_{i-1}^*} \mid \mathbf{n}_{1:i-1}),$$

which amounts to resampling all  $J$  particles with replacement from the set  $(\tau, z)_{1:N_{i-1}^*}^{(1:J)}$ , with respective probabilities  $W_{i-1}^{(1:J)}$ . The particles are then propagated to the current time increment by generating

$$(\tau, z)_{N_{i-1}^*+1:N_i^*}^{(j)} \sim Q(d(\tau, z)_{N_{i-1}^*+1:N_i^*} \mid (\tilde{\tau}, \tilde{z})_{1:N_{i-1}^*}^{(j)}, \mathbf{n}_{1:i}),$$

and appending the value to  $(\tilde{\tau}, \tilde{z})_{1:N_{i-1}^*}^{(j)}$ , for each  $j = 1, \dots, J$ . Finally, the particles are updated to a sample from the filtering distribution using Bayes'

theorem, by respectively assigning each the weight

$$w_i^{(j)} = p(\mathbf{n}_i \mid (\tau, z)_{1:N_i^*}^{(j)}, \mathbf{n}_{1:i-1}) \\ \times \frac{P(d(\tau, z)_{N_{i-1}^*+1:N_i^*} \mid (\tilde{\tau}, \tilde{z})_{1:N_{i-1}^*}^{(j)}, \mathbf{n}_{1:i-1})}{Q(d(\tau, z)_{N_{i-1}^*+1:N_i^*} \mid (\tilde{\tau}, \tilde{z})_{1:N_{i-1}^*}^{(j)}, \mathbf{n}_{1:i})} \Big|_{(\tau, z)_{N_{i-1}^*+1:N_i^*} = (\tau, z)_{N_{i-1}^*+1:N_i^*}^{(j)}}. \quad (2)$$

The desired approximations are again found from (1) to be

$$\hat{P}(d(\tau, z)_{1:N_i^*} \mid \mathbf{n}_{1:i}) = \sum_{j=1}^J W_i^{(j)} \delta_{(\tau, z)_{1:N_i^*}^{(j)}}(d(\tau, z)_{1:N_i^*}), \\ \hat{p}(\mathbf{n}_i \mid \mathbf{n}_{1:i-1}) = \frac{1}{J} \sum_{j=1}^J w_i^{(j)}.$$

The likelihood estimate is the product of the estimated marginal likelihood factors,

$$\hat{L}(\theta) = \prod_{i=1}^I \hat{p}(\mathbf{n}_i \mid \mathbf{n}_{1:i-1}).$$

A proof that  $\hat{L}(\theta)$  is unbiased is presented in [Chen et al. \(2025\)](#). The use of a guided particle filter avoids producing particles that disagree with the observed data, which may result in many particles with zero weight and eventual degeneracy of the SMC algorithm ([Chopin and Papaspiliopoulos, 2020](#)). We choose to propose event times using the ordered uniform distribution, due both to its simplicity in expression and desirable numerical properties. Formally, define the reference measure  $\mu$  on  $(\mathcal{M}, \mathcal{B}(\mathcal{M}))$  by

$$\mu(A) = \sum_{m=1}^M \delta_m(A), \quad A \in \mathcal{B}(\mathcal{M}).$$

Let  $n_i^* = \sum_{m=1}^M n_{i,m}$  be the total number of events observed on  $(t_{i-1}, t_i]$ . Define the set

$$\mathcal{M}_{\mathbf{n}_i} = \left\{ \mathbf{v} \in \mathcal{M}^{n_i^*} : \sum_{k=1}^{n_i^*} \mathbb{1}\{v_k = m\} = n_{i,m}, \text{ for all } m \in \mathcal{M} \right\},$$

which contains all combinations of event types that agree with the observation, and the set  $\mathcal{T}_i = \{t_{i-1} < \tau_{N_{i-1}^*+1} < \dots < \tau_{N_i^*} < t_i\}$ . We generate  $n_i^*$  event times from the ordered uniform distribution on  $(t_{i-1}, t_i]$ , then independently draw an event type vector from  $\mathcal{M}_{\mathbf{n}_i}$  with equal probability. It follows that

$$Q(d\tau_{N_{i-1}^*+1:N_i^*}, dz_{N_{i-1}^*+1:N_i^*} | \mathbf{n}_i) = Q(dz_{N_{i-1}^*+1:N_i^*} | \mathbf{n}_i) Q(d\tau_{N_{i-1}^*+1:N_i^*} | \mathbf{n}_i),$$

where

$$Q(d\tau_{N_{i-1}^*+1:N_i^*} | \mathbf{n}_i) = \frac{n_i^*!}{(t_i - t_{i-1})^{n_i^*}} \mathbb{1}_{\mathcal{T}_i}(\tau_{N_{i-1}^*+1:N_i^*}) d\tau_{N_{i-1}^*+1:N_i^*},$$

and

$$Q(dz_{N_{i-1}^*+1:N_i^*} | \mathbf{n}_i) = \frac{\prod_{m=1}^M n_{i,m}!}{n_i^*!} \mathbb{1}_{\mathcal{M}_{\mathbf{n}_i}}(z_{N_{i-1}^*+1:N_i^*}) \mu(dz_{N_{i-1}^*+1:N_i^*}).$$

Since the proposal does not dominate the predictive distribution for a given time  $t_i$ , the SMC procedure does not produce a valid estimate of the predictive distribution.

For the numerator of the weights in (2), *Proposition 7.3.III* in [Daley and Vere-Jones \(2003\)](#) gives

$$\begin{aligned} P(d(\tau, z)_{N_{i-1}^*+1:N_i^*} | (\tau, z)_{1:N_{i-1}^*}, \mathbf{n}_{1:i-1}) &= e^{-\int_{t_{i-1}}^{\tau_{N_i^*} \vee t_{i-1}} \lambda^*(t) dt} \prod_{k=N_{i-1}^*+1}^{N_i^*} \lambda_{z_k}(\tau_k) \\ &\times \mathbb{1}_{\mathcal{T}_i}(\tau_{N_{i-1}^*+1:N_i^*}) d\tau_{N_{i-1}^*+1:N_i^*} \mu(dz_{N_{i-1}^*+1:N_i^*}). \end{aligned}$$

Furthermore,

$$p(\mathbf{n}_i | (\tau, z)_{1:N_i^*}, \mathbf{n}_{1:i-1}) = e^{-\int_{\tau_{N_i^*} \vee t_{i-1}}^{t_i} \lambda^*(t) dt} \mathbb{1}_{\mathcal{M}_{\mathbf{n}_i}}(z_{N_{i-1}^*+1:N_i^*}).$$

Combining these expressions, the weight  $w_i^{(j)}$  will evaluate to

$$w_i^{(j)} = \frac{\left[ \prod_{k=N_{i-1}^*+1}^{N_i^*} \lambda_{z_k}(\tau_k^{(j)}) \right] e^{-\int_{t_{i-1}}^{t_i} \lambda^*(t) dt}}{\prod_{m=1}^M n_{i,m}! / (t_i - t_{i-1})^{n_i^*}}.$$

Note that in practice, weights are computed on a logarithmic scale. Letting  $G_{m,p}(\cdot)$  be the anti-derivative of the excitation function  $g_{m,p}$ ,  $m, p \in \mathcal{M}$ , the relevant integral is found to be

$$\begin{aligned} \int_{t_{i-1}}^{t_i} \lambda^*(t) dt &= \int_{t_{i-1}}^{t_i} \nu(t) dt + \sum_{m=1}^M \sum_{k=1}^{N_i^*} G_{m,z_k}(t_i - \tau_k) \\ &\quad - \sum_{m=1}^M \sum_{k=1}^{N_{i-1}^*} G_{m,z_k}(t_{i-1} - \tau_k). \end{aligned} \quad (3)$$

A derivation is presented in [A.1](#). In the case where the offspring densities  $h_{m,p}$ ,  $m, p \in \mathcal{M}$  each correspond to the density of an exponential random variable, the excitation component of the intensity process of the MHP is Markovian ([Oakes, 1975](#)). Simplifications can then be made to compute relevant quantities in the SMC algorithm, allowing for speed improvements and reduced storage costs. See [A.2](#) for details.

### 2.3 Parameter Estimation

We will now provide some rationale for the estimation procedure. For more details, see [Chen et al. \(2025\)](#). Assuming that the log-likelihood function is sufficiently regular, then for a large number of intervals,  $T$ , we have the approximation

$$\log L(\theta) = \log p_\theta(\mathbf{n}_{1:I}) \approx \log p_{\hat{\theta}}(\mathbf{n}_{1:I}) - \frac{1}{2}(\theta - \hat{\theta})^\top (-H(\hat{\theta}))(\theta - \hat{\theta}),$$

where  $H(\theta)$  is the Hessian of the log-likelihood and  $\hat{\theta}$  is the MLE of the observation. The likelihood function therefore satisfies an approximate proportionality relation of the form

$$L(\theta) \propto \exp\left(\frac{1}{2}(\theta - \hat{\theta})^\top (-H(\hat{\theta}))(\theta - \hat{\theta})\right),$$

which is a Gaussian density with respect to the Lebesgue measure. It follows that, if the log-likelihood is sufficiently regular, the distribution over the parameter space  $\Theta$  will be asymptotically Gaussian, with mean  $\hat{\theta}$  and covariance matrix  $H^{-1}(\hat{\theta})$ . If the likelihood were explicitly available, an approximation to the MLE and Hessian could be obtained by using Markov

Chain Monte Carlo (MCMC) to sample from  $L(\theta)$ , then taking the mean and variance of the resulting sample.

The Metropolis-Hastings algorithm is an appropriate method for constructing a Markov chain to approximate  $L(\theta)$ , as the likelihood is only known up to a constant of proportionality. Given the current state of the chain is  $\theta$ , we pick the proposal distribution  $Q(d\theta' | \theta)$  to be Gaussian with mean  $\theta$  and variance  $\delta$ . This is symmetric and dominates the target distribution. Taking a draw  $\theta' \sim Q(d\theta' | \theta)$ , we accept  $\theta'$  as the new state of the chain with probability  $L(\theta')/L(\theta)$ , else we reject and remain at  $\theta$ .

Since we cannot evaluate the likelihood function exactly when working with aggregated data, we instead use a PMMH algorithm ([Andrieu and Roberts, 2009](#)). This method functions identically to the typical Metropolis-Hastings method described, but replaces the likelihood  $L(\theta)$  with the SMC estimate  $\hat{L}(\theta)$ . This is justified due to the unbiasedness of the SMC estimator. It is important that, when implementing the algorithm, the value  $\hat{L}(\theta)$  is not recalculated each time the acceptance probability  $L(\theta')/L(\theta)$  is calculated - it should be done only once, with the value reused ([Andrieu and Roberts, 2009](#)). [Chen et al. \(2025\)](#) provide a proof that the stationary distribution of a Markov chain constructed using the PMMH method will yield the true likelihood  $L(\theta)d\theta$  as its stationary distribution. The result carries easily to the multivariate Hawkes process and is thus omitted.

### 3 Simulation Studies

In this section, numerical experiments are conducted to verify the accuracy of the proposed SMC procedure in likelihood approximation. Then, the ordered uniform proposal distribution used in our method is compared numerically to the Poisson proposals used by [Chen et al. \(2025\)](#). The performance of the estimators derived from the PMMH-MCMC algorithm is assessed on simulated sample paths, with a comparison made to the MCEM estimators of [Shlomovich et al. \(2022a\)](#).

#### 3.1 SMC Estimate of the Likelihood

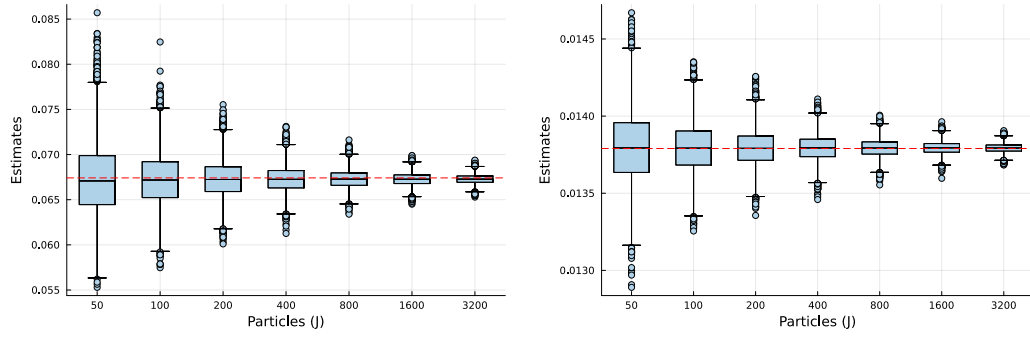
We now provide two experiments to verify the validity of the SMC algorithm. First, consider a bivariate Hawkes process with exponential excitation kernels  $h_{i,j}(t) = \frac{1}{\beta_{ij}}e^{-t/\beta_{ij}}$ . The background intensity vector is  $\nu = (1, 1)$ , and

the excitation parameters are  $\beta_{ij} = 0.5$  for any combination of  $i, j \in \{1, 2\}$ . Take the branching ratio matrix  $\eta$  to have diagonal entries of 0.6 and off-diagonal entries of 0.4. Define the event  $A := \{N_1(0, 1] = 1, N_2(0, 1] = 1\}$ , that is, precisely one event of each type in the first unit of time. A standard Monte Carlo approach involving the simulation and inspection of  $10^6$  samples yields the estimate 0.0674 for  $P(A)$ . Figure 1a displays 10,000 SMC estimates of  $P(A)$ , with varying number of particle  $J$ . The mean estimate is close to the Monte Carlo estimate even for low  $J$  values, with the empirical bias and variance decreasing in  $J$ .

Next, consider again a bivariate Hawkes process with baseline intensity vector  $\nu$  and branching ratio matrix  $\eta$  as before, but now characterised by gamma offspring densities  $h_{i,j}(t) = t^{\kappa_{ij}-1} e^{-t/\delta_{ij}} / (\Gamma(\kappa_{ij}) \delta_{ij}^{\kappa_{ij}})$ , with shape and scale parameters given respectively by

$$\kappa = \begin{pmatrix} 2 & 3 \\ 3 & 2 \end{pmatrix}, \quad \delta = \begin{pmatrix} 1 & 2 \\ 2 & 1 \end{pmatrix}.$$

Define the event  $B := \{N_1(0, 1] = N_1(1, 2] = N_2(0, 1] = N_2(1, 2] = 1\}$ . The standard Monte Carlo approach estimates  $P(B)$  to be 0.01379 using  $10^6$  sample paths. Figure 1b shows convergence of the mean SMC estimate of  $P(B)$  to the Monte Carlo estimate, and reduction in the variance as the number of particles increases.



(a)  $P(A)$ , MHP with exponential kernel. (b)  $P(B)$ , MHP with gamma kernel.

Figure 1: Box plots of 10,000 SMC estimates of  $P(A)$  and  $P(B)$  respectively, with  $A$  and  $B$  defined in Section 3.1. The Monte-Carlo estimates are marked by the red dashed lines.

### 3.2 Evaluation of the Proposal Distribution

Our proposed SMC algorithm implements an ordered uniform proposal distribution for sampling latent event times, which we now compare to the finite distributions of a Poisson process used in [Chen et al. \(2025\)](#). Consider a representative observation interval  $(t_{i-1}, t_i]$ , with unobserved event times  $\tau_{N_{i-1}^*+1:N_i^*}$  and types  $z_{N_{i-1}^*+1:N_i^*}$ . The Poisson proposal method is designed such that proposed times  $\tau_{N_{i-1}^*+1:N_i^*}$  are distributed according to the first  $n_i^*$  events of a homogeneous Poisson process on  $(t_{i-1}, \infty)$  with rate parameter  $\rho = \gamma_{0.95;n_i^*,1}/(t_i - t_{i-1})$ , taking  $\gamma_{0.95;n_i^*,1}$  to be the 0.95 quantile of the gamma distribution with shape parameter  $n_i^*$  and rate 1. [Chen et al. \(2025\)](#) arbitrarily select  $\gamma_{0.95;n_i^*,1}$  as this achieves a probability of 0.95 that the proposed event times will fall within the  $i^{\text{th}}$  observation window. Event types are then assigned from the multinomial distribution, as described in Section 2.2. This is a natural multivariate extension of the univariate method of [Chen et al. \(2025\)](#). In practice, event times are generated by sampling  $n_i^*$  exponential random variables with rate  $\rho$  and computing their cumulative sum.

For the ordered uniform proposals, we begin by sampling the first  $n_i^* + 1$  times of the Poisson process with rate 1, followed by a simple transformation to return  $n_i^*$  ordered uniforms on  $(t_{i-1}, t_i]$ . See sections V.2 and V.3 of [Devroye \(1986\)](#) for relevant proofs and discussion of computational complexity. The computational time of both methods is linear in the number of particles. One advantage of the ordered uniform distribution is that proposals are guaranteed to agree with observations, whereas with Poisson proposals, on average 5% of the particles disagree with the observations, resulting in the assignment of zero weights and a loss of efficiency.

The ordered uniform proposal method also demonstrates significantly lower variance in the SMC likelihood estimates compared to using Poisson proposals. Using a single simulated sample path of the MHP with censoring time  $T = 200$  and observation windows of width  $\Delta = 0.5$ , we estimate the log-likelihood at the true parameter 500 times using  $J \in \{50, 100, 200\}$  particles. See Section 3 for full details on the simulated sample path. The results are shown in Figure 2. The ordered uniform proposal is significantly more efficient, with empirical variance a factor of 200 to 250 times smaller than that of the Poisson proposals. Such efficiency gains allow the PMMH chain to be run with fewer particles (by the order of  $10^3$  or  $10^4$ ) while maintaining accurate SMC likelihood estimates. Accurate SMC estimates reduce the chance of an unusually high likelihood estimate causing the PMMH chain

to stay in place for extended periods. Given the increased demands of estimating many parameters in the multivariate setting, this efficiency gain is crucial for the practicability of the PMMH estimation method.

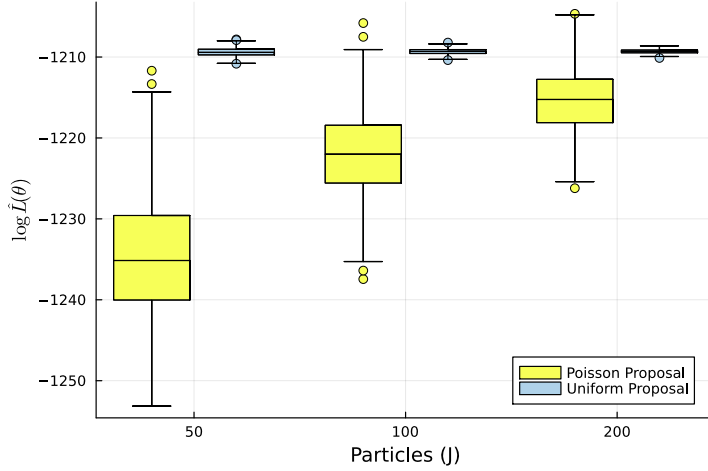


Figure 2: Box plots of 500 SMC estimates of  $\log L(\theta)$ , using uniform and Poisson proposals.

### 3.3 MLE Approximation via PMMH-MCMC

This section is devoted to assessing the finite-sample performance of the PMMH-MCMC estimator of the model parameters. A bivariate Hawkes process with exponential kernel and parameters

$$\nu = \begin{pmatrix} 0.8 \\ 1.0 \end{pmatrix}, \quad \eta = \begin{pmatrix} 0.6 & 0.3 \\ 0.25 & 0.5 \end{pmatrix}, \quad \beta = \begin{pmatrix} 0.5 & 0.5 \\ 0.75 & 0.75 \end{pmatrix}$$

is simulated from the origin to time  $T = 200$ . The true parameter  $\beta$  satisfies  $\beta_{1,1} = \beta_{1,2} =: \beta_1$  and  $\beta_{2,1} = \beta_{2,2} =: \beta_2$ , reflecting the model assumption that all type 1 and type 2 offspring events have, respectively, equal mean waiting time, regardless of the type of the parent event.

We simulate  $S = 500$  sample paths, with events aggregated into observation periods of width  $\Delta \in \{0.1, 0.5, 1.0, 5.0\}$ . The censoring time  $T = 200$  was chosen to yield an average of approximately 2,000 events in a sample path. The PMMH algorithm is run for  $N = 30,000$  iterations, with the

approximate MLE of each parameter taken to be the median of the resulting sample. The upper and lower 2.5 percentile points define the approximate 95% Wald confidence interval, with the width of the interval divided by  $2\Phi^{-1}(0.975)$  to be the estimated standard error of the approximate MLE. The case of  $\Delta = 0$  is also considered, corresponding to knowledge of exact event times, for which the log-likelihood is explicitly known. The MLE is therefore available via minimisation of the negative log-likelihood function, with estimates of the standard error obtained by taking the square roots of the diagonal entries of the inverse Hessian matrix. The MLE is computed numerically using the `optimize` function from the `julia` package `Optim`. The Hessian is also computed numerically in `julia`, using the `hessian` function from the `ForwardDiff` package. Letting  $n_1$  and  $n_2$  be the total number of type 1 and type 2 events, respectively, each chain is initialised at  $\nu_0 = (n_1/2T, n_2/2T)$ , which naively assumes that half of the observations are background events. The initial branching ratio matrix is given by  $(\eta_0)_{1,1} = (\eta_0)_{2,2} = 0.6$  and  $(\eta_0)_{1,2} = (\eta_0)_{2,1} = 0.2$ , chosen such that the self-excitation effects are stronger than the cross-excitation effects. All  $\beta_{i,j}$  terms are initialised at 1. Estimates are also computed using only the data to a shortened censoring time of  $T = 100$  to assess the improvement in estimation quality with additional data.

The results are summarised in Table 1, which reports the mean approximate MLE over the 500 simulated paths (Est), the empirical standard error of the 500 estimates (SE), the mean of the standard error estimates computed using the approximate confidence interval as previously described ( $\widehat{SE}$ ) and the empirical coverage probability of the approximate confidence intervals (CP). Identical experiments are also conducted on the set of 500 sample paths, but without enforcing the condition that  $\beta_{1,2} = \beta_{1,1}$  and  $\beta_{2,1} = \beta_{2,2}$ , which increases the difficulty of the inference problem. The results are summarised in Table 4 in B.

The results in Table 1 suggest that for aggregation levels  $\Delta \in \{0.1, 0.5\}$ , the PMMH algorithm performs similarly in terms of empirical bias and standard error to the MLE computed for  $\Delta = 0$ , across all parameters. Using our PMMH method with SMC, very little information loss is incurred for low levels of aggregation. The PMMH estimator appears to produce lower biases, but slightly higher standard errors than the MLE, for these low aggregation levels. The greater bias of the exact MLE calculations appears to be due to a few outlier sample paths, which, in this case, the PMMH algo-

Table 1: Summary of results from PMMH-MCMC Simulation Experiment.

	$\nu_1$	$\nu_2$	$\eta_{1,1}$	$\eta_{1,2}$	$\eta_{2,1}$	$\eta_{2,2}$	$\beta_1$	$\beta_2$
True Parameters	0.8	1.0	0.6	0.3	0.25	0.5	0.5	0.75
$T = 100$	Est	0.885	1.120	0.567	0.311	0.263	0.452	0.499
	SE	0.358	0.350	0.079	0.089	0.083	0.104	0.104
	$\widehat{SE}$	0.317	0.338	0.075	0.086	0.079	0.099	0.102
$\Delta = 0$	CP	0.930	0.946	0.924	0.950	0.950	0.920	0.924
$T = 200$	Est	0.845	1.059	0.584	0.304	0.256	0.477	0.493
	SE	0.226	0.265	0.052	0.057	0.054	0.069	0.070
	$\widehat{SE}$	0.226	0.245	0.052	0.059	0.053	0.069	0.070
	CP	0.946	0.948	0.944	0.966	0.956	0.934	0.930
$T = 100$	Est	0.835	1.111	0.581	0.297	0.249	0.460	0.528
	SE	0.440	0.418	0.088	0.119	0.128	0.145	0.118
	$\widehat{SE}$	0.323	0.359	0.080	0.093	0.086	0.110	0.118
$\Delta = 0.1$	CP	0.900	0.938	0.938	0.900	0.878	0.904	0.942
$T = 200$	Est	0.818	1.045	0.589	0.301	0.253	0.483	0.505
	SE	0.249	0.279	0.053	0.062	0.061	0.076	0.075
	$\widehat{SE}$	0.235	0.254	0.054	0.064	0.057	0.073	0.076
	CP	0.948	0.942	0.944	0.958	0.952	0.932	0.948

rithm is more robust to. A minor drop in performance relative to the MLE is observed for  $\Delta = 1.0$ , though the results are still accurate. As expected, a more significant increase in the standard error of the estimates is observed for  $\Delta = 5.0$ , corresponding to an average of 50 events per observation period, which is a fairly extreme level of aggregation. It may be that  $\Delta = 5.0$  is too large an aggregation level relative to the censoring time and number of events to justify the asymptotic Gaussian approximation. In general, the biases of the estimates are negligible in comparison to their respective standard errors, which is aligned with the behaviour of the MLE. Furthermore, the standard errors change by a factor of approximately  $1/\sqrt{2}$  when the censoring time is doubled, which is to be expected of a method that converges at rate  $\sqrt{T}$ . Figure 8 in B presents the standard error on censoring times  $T \in \{100, 200, 400\}$ .

		Est	0.830	1.122	0.581	0.297	0.249	0.455	0.528	0.840
		SE	0.464	0.419	0.096	0.141	0.133	0.154	0.127	0.356
		$\widehat{SE}$	0.331	0.361	0.086	0.102	0.089	0.114	0.132	0.274
		CP	0.894	0.940	0.936	0.892	0.884	0.888	0.948	0.930
$\Delta = 0.5$		Est	0.823	1.049	0.589	0.300	0.253	0.481	0.504	0.773
		SE	0.260	0.283	0.059	0.077	0.066	0.085	0.082	0.173
		$\widehat{SE}$	0.242	0.254	0.059	0.072	0.061	0.076	0.085	0.162
		CP	0.946	0.936	0.944	0.950	0.934	0.934	0.956	0.948
$\Delta = 1.0$		Est	0.851	1.111	0.586	0.282	0.256	0.447	0.537	0.826
		SE	0.494	0.439	0.111	0.173	0.152	0.172	0.151	0.375
		$\widehat{SE}$	0.343	0.362	0.094	0.115	0.096	0.120	0.154	0.304
		CP	0.884	0.940	0.932	0.864	0.858	0.880	0.938	0.918
$\Delta = 5.0$		Est	0.823	1.047	0.592	0.294	0.253	0.481	0.512	0.771
		SE	0.294	0.285	0.069	0.103	0.079	0.095	0.098	0.200
		$\widehat{SE}$	0.251	0.258	0.065	0.084	0.068	0.083	0.099	0.180
		CP	0.932	0.944	0.934	0.918	0.932	0.916	0.960	0.948
$\Delta = 10.0$		Est	0.902	1.074	0.558	0.302	0.318	0.385	0.788	0.924
		SE	0.568	0.564	0.174	0.246	0.200	0.197	0.567	0.517
		$\widehat{SE}$	0.327	0.344	0.107	0.123	0.103	0.114	0.282	0.403
		CP	0.798	0.840	0.844	0.780	0.764	0.764	0.800	0.902
$\Delta = 20.0$		Est	0.882	0.984	0.608	0.262	0.300	0.438	0.732	0.853
		SE	0.382	0.392	0.108	0.156	0.133	0.142	0.213	0.320
		$\widehat{SE}$	0.212	0.218	0.066	0.076	0.065	0.075	0.152	0.212
		CP	0.745	0.788	0.784	0.699	0.723	0.725	0.559	0.826

### 3.4 Comparison with Monte Carlo Expectation-Maximisation

A recently published alternative method of inference for the discretely observed MHP is the MCEM algorithm of [Shlomovich et al. \(2022a\)](#). The MCEM estimators are compared to our PMMH estimators using the 500 simulated sample paths from Section 3.3, for the case  $T = 200$ . We note that the MCEM method is applicable only to data with equal sized observation windows and hence can be used in this setting. The MCEM estimators are computed using the `Matlab` code released as supplement to [Shlomovich et al. \(2022a\)](#)<sup>1</sup>, which we implement using the specifications in their simulation study. *Sequential* sampling is used as it is reportedly the least biased of the two methods proposed by [Shlomovich et al. \(2022a\)](#). The `Matlab` code was edited to enforce the constraints  $\beta_{1,1} = \beta_{1,2}$  and  $\beta_{2,1} = \beta_{2,2}$  in their numerical optimisation step, so as to ensure a fair comparison.

Figure 3 shows the comparison for each  $\Delta$  value. It is clear that, even for a small level of aggregation, the MCEM estimators have a large bias, with the body of some boxplots lying entirely away from the true parameter. Estimates of the excitation parameters have significantly greater variance than the corresponding PMMH estimates, for low levels of aggregation. Overall, the PMMH method outperforms the MCEM method based on mean-squared error. The two methods have comparable variance for  $\Delta = 5.0$ , though the PMMH estimates remain less empirically biased. The significant bias in the MCEM method may be driven by their deterministic selection procedure, with latent event times chosen as the mode of a proposal distribution, as opposed to taking a weighted average over a sample from the proposal. The bias from this approach carries through to the parameters, and behaves unpredictably as  $\Delta$  is varied.

## 4 Analysis of Terror Attack Data

The modelling of terrorist activity is an important application area for the MHP, with data for a given region typically reported in daily counts. We now apply our estimation procedure to a cross-country analysis of terrorist activity using the [GTD \(2022\)](#)<sup>2</sup>, a highly comprehensive dataset on worldwide terrorism events. Our method avoids the discrete time modelling and data

---

<sup>1</sup>Available at the following link: [MCEM\\_Multivariate\\_Hawkes](#)

<sup>2</sup>Available at the following link: <https://www.start.umd.edu/gtd/>

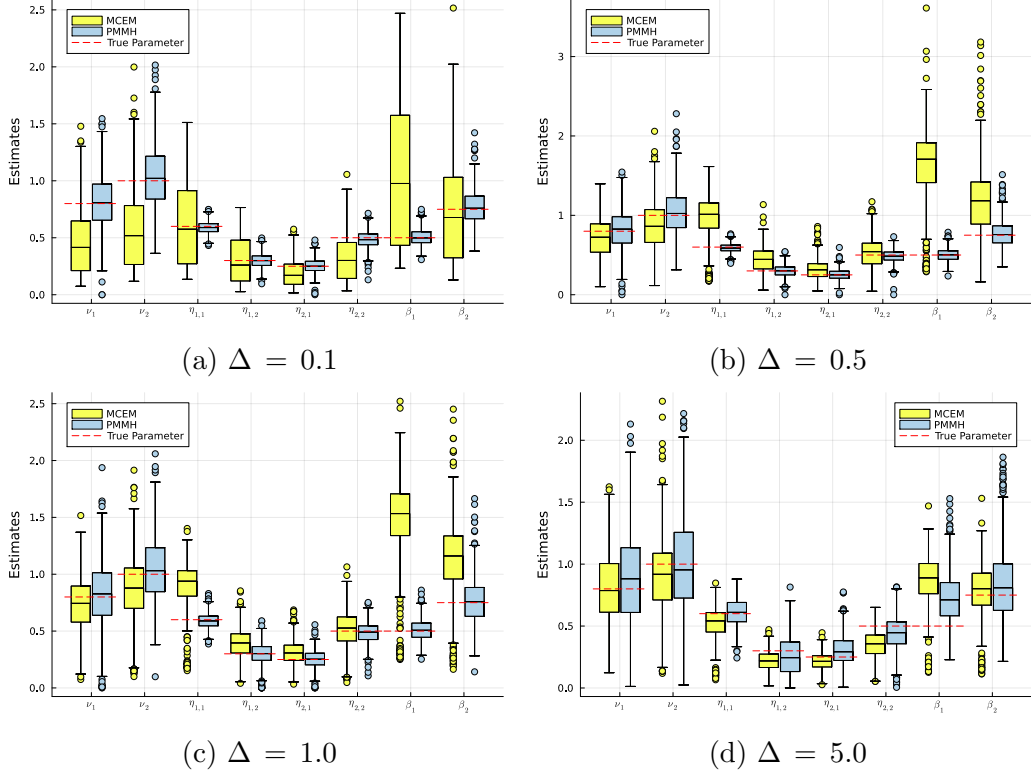


Figure 3: Comparison of MCEM and PMMH estimates on 500 sample paths.

augmentation approaches taken by many existing point process analyses of terrorism with aggregated data.

#### 4.1 Terrorism in Afghanistan and Pakistan

The United States of America (US) conducted a complete military withdrawal from Afghanistan over the period of March 9<sup>th</sup>, 2020, to August 30<sup>th</sup>, 2021 (Baldor, 2020; Zeidan, 2024). Since this time, the nation of Pakistan has reportedly seen a significant increase in terrorist activity, primarily attributed to the organisation *Tehreek-e-Taliban* (TTP) (Akhtar and Ahmed, 2023). The TTP is an organisation that operates along Pakistan's northwestern border with Afghanistan, formerly the Federally Administered Tribal Areas (FATA) of Pakistan (Abbas, 2008). The TTP originated as sympathisers to the Afghan Taliban, but since the mid 2000s, they have

held their own command structure, independent of the Afghan Taliban (Abbas, 2008). The group experienced fragmentation through the 2010s decade, though showed signs of a resurgence in the late 2010s (Sayed and Hamming, 2023). The rise of terrorist activity in Pakistan has garnered significant media attention through 2023 and early 2024, with Pakistan-Afghanistan tensions consistently identified as causal factors in Pakistan's terrorism spike (Hussain, 2023; Aziz, 2023; Hussain, 2024). An official statement by the US Department of State (2024) outlines an ongoing joint effort between the US and Pakistan to counter the rising terrorism in the nation, identifying as key groups of interest the TTP and ISIS-Khorasan, another militant organisation operating across Afghanistan and Pakistan (Doxsee et al., 2021).

Given the interest in terrorist activity across Pakistan and Afghanistan, we model terrorist events in the two nations during the US withdrawal from Afghanistan with a MHP, obtaining estimates via our proposed PMMH procedure. The temporal clustering of terrorism in Afghanistan has been studied extensively (Zammit-Mangion et al., 2012; Rieber-Mohn and Tripathi, 2021; Jun and Cook, 2024), suggesting that the nation is an appropriate candidate for a Hawkes process model. To the best of our knowledge, Pakistan has not been the subject of such statistical analysis. Comprehensive data on terrorist activity is available from the GTD (2022) through the period March 9<sup>th</sup>, 2020 to June 30<sup>th</sup>, 2021. Insights into the dynamics of the two nations during this time period may be drawn from our estimation.

#### 4.1.1 Preliminary Analysis

There has been a marked increase in the number of terrorist events in Pakistan and Afghanistan over the period 1970 - 2020, as seen in Figure 4. Both nations show a similar trajectory, with few events until the late 1990s and early 2000s, after which an exponential increase in terrorism is observed, attributable either to an actual rise in terrorist activity, or a significant increase in reporting of terrorism. Pakistan displays some taper in events in the later part of the 2010s decade. It is clear that a MHP model for both nations over any extended period would require the estimation of a non-linear baseline rate.

Restricting our attention to the period coinciding with the US exit from Afghanistan, we see a far more consistent trend in the data, shown by the red line of cumulative event counts in Figure 6. This motivates the choice of a constant baseline intensity function in line with the work of Tench et al.

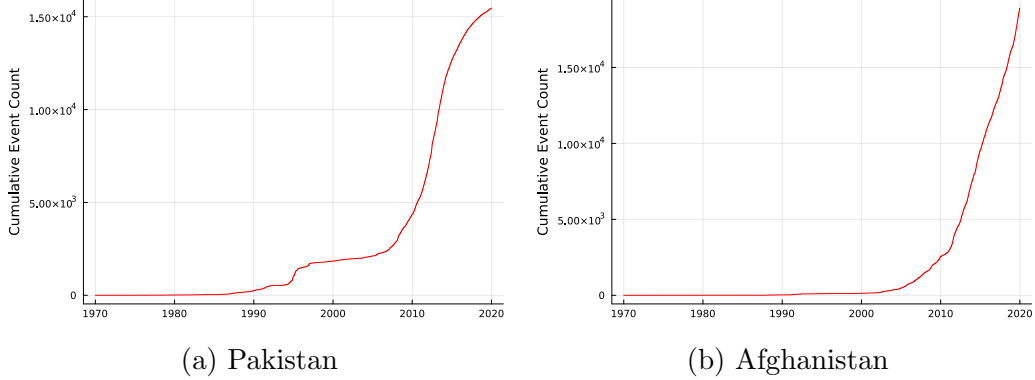


Figure 4: Cumulative number of terror attacks in Pakistan and Afghanistan, 1970 - 2020.

(2016) and Porter and White (2012). Figure 5 shows the daily event counts in both Pakistan and Afghanistan. In total, Pakistan experienced 361 terrorist attacks over this time period, averaging 0.816 events per day, whereas Afghanistan experienced 3,588 attacks, an average of 7.78 events per day. Terrorism in Pakistan shows fairly consistent behaviour; the majority of observations are either 0 or 1 event, with few intermittent spikes, and a maximum of 5 events in a single day attained four times. Afghanistan has far more variability, with most counts sitting in the range of 3 to 10 per day, with frequent spikes. The maximum of 21 events per day is observed three times.

#### 4.1.2 Model and Estimation

For a bivariate Hawkes process,  $\mathbf{N}(t)$ , let an event in Afghanistan be considered type 1, denoted by the indicator  $z_i = 1$ , and an event in Pakistan be type 2, denoted by  $z_i = 2$ . The GTD (2022) contains the sample paths of terrorism events in both countries, observed daily. We therefore have an initial time of  $t_0 = 0$ , censoring time of  $T = 461$ , with the  $i^{\text{th}}$  observation period defined by  $(t_{i-1}, t_i] = (i-1, i]$ . The model is specified with a constant baseline, and, following existing works on Hawkes process models of terrorist activity (Tench et al., 2016; Zhou and Papadogeorgou, 2023), an exponential offspring kernel. As in Section 3.3, we enforce the condition  $\beta_{1,1} = \beta_{1,2} =: \beta_1$  and  $\beta_{2,1} = \beta_{2,2} =: \beta_2$  for the mean waiting time for offspring events in each nation, respectively.

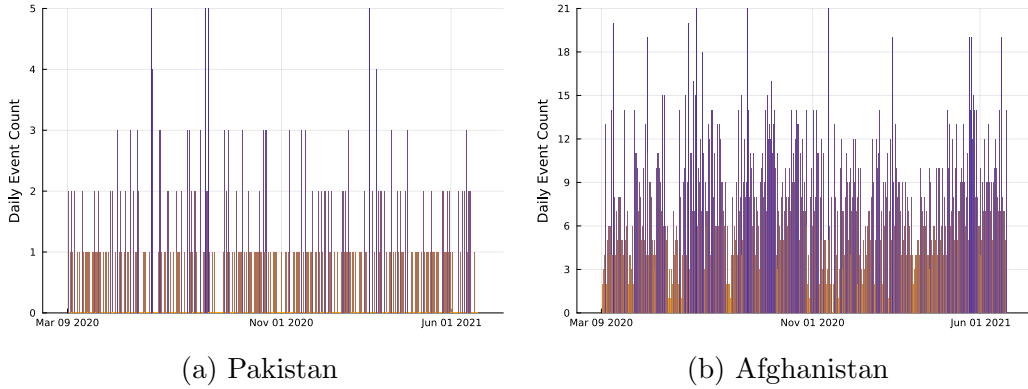


Figure 5: Daily terror attack counts in Pakistan and Afghanistan during US Exit.

The PMMH-MCMC algorithm was run for  $N = 30,000$  iterations with a jump size of  $\delta = 0.12$ . Inspection of the trace plots of the MCMC chain shows good mixing (Figure 10). The first 3,000 iterations are excluded as the burn-in period, with the median of the remaining 27,000 iterations taken to be the approximate MLE. The approximated MLE values and respective standard error estimates are displayed in Table 2. Multiple runs of the PMMH-MCMC algorithm were performed with different initial parameters, all of which converged to approximately the same location. Also included in Table 2 are estimates of the data using the MCEM method (Shlomovich et al., 2022a) and a naive method along the lines of Tench et al. (2016), whereby the MLE is calculated on exact event times placed at each observation time  $t_i$ , with a normally distributed perturbation. As expected, this approach is in complete disagreement with other estimates and does not produce estimates that reflect the observed data.

Figure 6 compares the observed count data of terrorism events across both nations to 500 sample paths simulated from the approximate MLE. The dashed black lines mark the upper and lower 95% quantiles of the simulated paths, with the observed data falling within these bounds, suggesting that the MHP with our proposed estimation procedure is capable of producing estimates that agree with the observations. An equivalent comparison using the MCEM estimates is given in Figure 9, which highlights the negative bias in the estimation of the background rate and branching ratios.

A few key insights can be taken from the estimates. Firstly, over the

Table 2: Approximate MLE and SE, Afghanistan and Pakistan during US exit period.

	$\nu_1$	$\nu_2$	$\eta_{1,1}$	$\eta_{1,2}$	$\eta_{2,1}$	$\eta_{2,2}$	$\beta_1$	$\beta_2$
Est	2.860	0.646	0.611	0.156	0.014	0.058	1.351	3.291
$\widehat{SE}$	0.568	0.107	0.071	0.146	0.013	0.049	0.398	14.0
MCEM	1.266	0.481	0.271	0.013	0.001	0.091	0.353	1.39
Naive	0.977	0.101	0.802	0.081	0.695	0.107	0.006	0.006

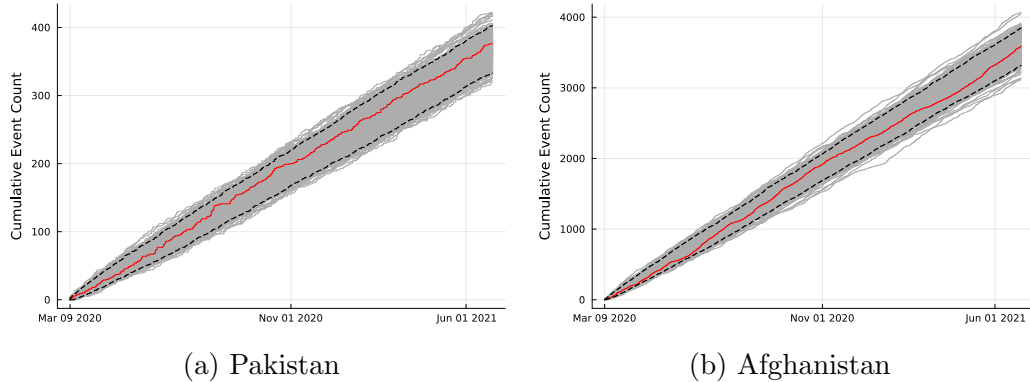


Figure 6: Observed cumulative number of terrorist events in Pakistan and Afghanistan compared to  $S = 500$  paths simulated from  $\hat{\theta}$ . Dashed black lines indicate upper and lower 95% quantiles and red lines indicate observed count data.

period of the US exit, Afghanistan saw significant self-excitation effects in terrorist activity, which agrees with previous work indicating that terrorism in the nation occurs in clusters (Zammit-Mangion et al., 2012; Rieber-Mohn and Tripathi, 2021; Jun and Cook, 2024). However, no significant cross-excitation was detected in the model, and Pakistan showed no significant self-excitation. Terrorism in the two countries therefore appears not to have been linked via a cross-excitation mechanism over this period. The difference in dynamics between the two nations is clear; events in Afghanistan are likely to trigger offspring events, whereas events in Pakistan carry minimal risk of triggering a short-term rise in terrorism. This analysis does not suggest that terrorism in the two nations is unrelated. We can only conclude that cross-

national excitation effects are unlikely to have been present. Note that the significant variability associated with  $\hat{\beta}_2$  is driven by the fact that  $\hat{\eta}_{2,1}$  and  $\hat{\eta}_{2,2}$  are very close to 0, rendering  $\beta_2$  weakly identifiable, and therefore should be taken only as an indication of lack of excitation effects in Pakistan.

Though the Pakistani Taliban (TTP) is thought to have an independent command and operational structure to the Afghan Taliban (Abbas, 2008), reports suggest that many TTP members operated alongside the Afghan Taliban through 2020-2021 as the Afghan Taliban retook control of Afghanistan (Sayed and Hamming, 2023). Our analysis suggests that, through the period of the US exit from Afghanistan, there may have been limited coordination of attacks between groups operating in each nation. Tench et al. (2016) came to similar conclusions in their analysis of terrorist attacks by the Provisional Irish Republican Army (PIRA) in Northern Ireland during *the Troubles*. The PIRA operated with command structures separated only by county lines, with insignificant cross-excitation observed, despite the relative proximity in comparison to our case study. However, with the Taliban now controlling Afghanistan and reportedly sympathetic to the objectives of the TTP (Sayed and Hamming, 2023), analysis of an up-to-date dataset will be required to gain an insight into whether any cross-excitation between the two nations has emerged in the years following the US exit from Afghanistan.

## 4.2 Longer-Term Analysis

As shown in Figure 4, the dynamics of terrorism in Afghanistan and Pakistan change over time. We now investigate whether cross-excitation effects exist between the two nations when a longer time period is considered by using the daily count data between January 1<sup>st</sup>, 2018, and June 30<sup>th</sup>, 2021. The cumulative observations are displayed in Figure 7. A slight concavity is clear in the event data for Pakistan, in contrast to a mild convexity for Afghanistan, which is accounted for by using a spline to model the background intensity. Specifically,  $\nu_1(t)$  and  $\nu_2(t)$  are order 2 B-splines with two knots each, at locations  $\{290, 798\}$  and  $\{240, 650\}$  respectively, determined from a visual assessment of the data. The final knot location of  $t = 798$  for  $\nu_1$  corresponds to the initiation of the US exit from Afghanistan. This was chosen to gain some indication of whether any change in the dynamics of terrorism occurred in the nation around this time. The assumption  $\beta_{1,1} = \beta_{1,2} =: \beta_1$  and  $\beta_{2,1} = \beta_{2,2} =: \beta_2$  is again imposed.

The approximate MLE and SE from 50,000 iterations of the PMMH al-

gorithm are presented in Table 3, with the first 10% of the chain removed as the burn-in period. The initial point of the chain was chosen based on multiple runs of the PMMH algorithm with different initial points, all of which converged to approximately the same location. We again simulate 500 comparative sample paths from the MLE, displayed in Figure 7. The model is clearly appropriate for modelling terrorist activity in Pakistan, and also fits well for Afghanistan.

Table 3: Approximate MLE and SE, Afghanistan and Pakistan, 2018 - 2021.

	$\nu_{1,1}$	$\nu_{1,2}$	$\nu_{1,3}$	$\nu_{1,4}$	$\nu_{2,1}$	$\nu_{2,2}$	$\nu_{2,3}$
Est	1.849	2.147	2.546	4.469	1.371	1.174	0.728
$\widehat{SE}$	0.216	0.191	0.190	0.310	0.150	0.083	0.061
	$\nu_{2,4}$	$\eta_{1,1}$	$\eta_{1,2}$	$\eta_{2,1}$	$\eta_{2,2}$	$\beta_1$	$\beta_2$
Est	0.746	0.527	0.131	0.004	0.082	0.422	0.069
$\widehat{SE}$	0.068	0.028	0.071	0.003	0.021	0.061	0.053

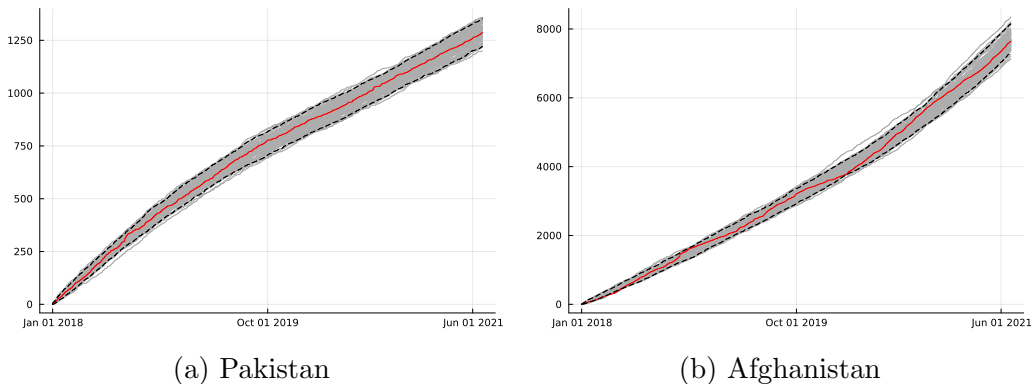


Figure 7: Observed cumulative number of terrorist events in Pakistan and Afghanistan compared to  $S = 500$  paths simulated from  $\hat{\theta}$ . Dashed blue lines mark spline knots, dashed black lines indicate upper and lower 95% quantiles, and red lines indicate observed count data.

New insights are revealed from the longer-term analysis. Self-excitation in Afghanistan remains high, with statistically significant self-excitation also detected in Pakistan over the time period. This indicates that clustering of

terrorism was present in Pakistan, though the magnitude of the effect is much lower than in Afghanistan. A cross-excitation effect of events in Pakistan on events in Afghanistan is also detected at the 95% level, captured by  $\hat{\eta}_{1,2}$ . Terrorism in Pakistan may therefore have had a minor triggering effect on terrorism in Afghanistan over the period. The estimate of  $\hat{\eta}_{2,1}$  remains near zero, with clear edge effects present in the sample histogram (Figure 13). We again take this as an indication of minimal cross-excitation from Afghanistan to Pakistan. The low values of  $\hat{\eta}_{2,1}$  and  $\hat{\eta}_{2,2}$  make  $\beta_2$  weakly identifiable, hence the erratic behaviour of the MCMC chain along this dimension (Figure 12). Finally, the difference  $\hat{\nu}_{1,4} - \hat{\nu}_{1,3} \approx 1.9$  suggests a distinct acceleration of the rate of terrorism during the US exit relative to the period prior. It is possible that the change in background dynamics was causally linked to the US exit, illustrating the need to utilise models with non-constant background rates to capture some of the complex social and political dynamics that underpin terrorism.

## 5 Discussion

This work contributes a methodology for analysing terrorist activity using discretely observed point process data, addressing limitations in existing approaches. Specifically, an unbiased SMC estimate of the intractable likelihood function is implemented, with parameter estimates for the MHP obtained from a PMMH-MCMC algorithm. Numerical evidence shows that our SMC algorithm, using the ordered uniform proposal distribution, outperforms a multivariate extension of the Poisson proposal distribution in [Chen et al. \(2025\)](#). In simulation experiments, our methodology produces statistically efficient estimators of the MHP under varying levels of aggregation and outperforms the competing MCEM method of [Shlomovich et al. \(2022a\)](#).

In application to terror attack data in Pakistan and Afghanistan, the PMMH estimates agree with the observed data and standard error estimates are provided, which are not available when using the MCEM algorithm. Our proposed methodology does not incur any loss of information from data augmentation and allows for continuous time modelling of terrorism events. Furthermore, the flexibility of the SMC and PMMH algorithms to handle non-constant baseline intensities enables the modelling of terrorism over long time periods with shifting background dynamics.

The estimators drawn from the PMMH algorithm are taken to be the

center of the invariant distribution of the MCMC sample. Though they have demonstrated good performance, we rely fundamentally on the assumption that the MLE is consistent and asymptotically normal to justify this choice. A proof detailing the conditions under which such properties hold will be pursued in other works. Theoretical treatments of SMC and PMMH methods in general contexts are also available (Del Moral, 2013; Andrieu et al., 2010). Limiting results for these algorithms are also of interest for future exploration.

Avenues for improving the computational efficiency of our method remain open. Fine tuning the choice of input parameters to the PMMH algorithm according to the advice in the literature (Doucet et al., 2015; Sherlock et al., 2015) may yield improvements. Recent works have proposed variants of the PMMH algorithm that improve performance in certain contexts, such as Deligiannidis et al. (2018), who correlate the SMC estimates in subsequent iterations of the MCMC chain to reduce computational time, or Middleton et al. (2020), who utilise coupled Markov chains run in parallel to eliminate burn-in bias. Whether such techniques are beneficial for estimating the discretely observed Hawkes process remains to be seen.

## Acknowledgements

This research has benefited from discussions with participants of the Point Process discussion group seminar series, especially Prof Yongtao Guan of the Chinese University of Hong Kong, Shenzhen.

## Funding

Lambe was supported by the Australian government research training program scholarship and the faculty top up scholarships from the School of Mathematics and Statistics, University of New South Wales Sydney. The Commonwealth of Australia (represented by the Department of Defence) supports this research through a Defence Science Partnerships agreement. This research was partially supported by the Australian Government through the Australian Research Council’s Discovery Projects funding scheme (project DP240101480). The views expressed herein are those of the authors and are not necessarily those of the Australian Government or the Australian Research Council.

# A Derivations

## A.1 Importance Weights

This section details the derivation of our expression for  $\log w_i^{(j)}$  in (3). Assuming that  $\tau_{N_i} > t_{i-1}$  for simplicity, we get

$$\int_{t_{i-1}}^{\tau_{N_i}} \lambda(s)ds = \nu(\tau_{N_i} - t_{i-1}) + \sum_{m=1}^M \int_{t_{i-1}}^{\tau_{N_i}} \varphi_m(s)ds.$$

For any given  $m \in \mathcal{M}$ , write

$$\int_{t_{i-1}}^{\tau_{N_i}} \varphi_m(s)ds = \int_{t_{i-1}}^{\tau_{N_{i-1}+1}} \varphi_m(s)ds + \sum_{K=N_{i-1}+2}^{N_i} \int_{\tau_{K-1}}^{\tau_K} \varphi_m(s)ds. \quad (4)$$

The first integral is

$$\begin{aligned} \int_{t_{i-1}}^{\tau_{N_{i-1}+1}} \varphi_m(s)ds &= \sum_{k=1}^{N_{i-1}} \int_{t_{i-1}}^{\tau_{N_{i-1}+1}} g_{m,z_k}(s - \tau_k)ds \\ &= \sum_{k=1}^{N_{i-1}} \{G_{m,z_k}(\tau_{N_{i-1}+1} - \tau_k) - G_{m,z_k}(t_{i-1} - \tau_k)\}. \end{aligned} \quad (5)$$

The remaining components of (4) are given by

$$\begin{aligned} \sum_{K=N_{i-1}+2}^{N_i} \int_{\tau_{K-1}}^{\tau_K} \varphi_m(s)ds &= \sum_{K=N_{i-1}+2}^{N_i} \sum_{k=1}^{K-1} \int_{\tau_{K-1}}^{\tau_K} g_{m,z_k}(s - \tau_k)ds \\ &= \sum_{K=N_{i-1}+2}^{N_i} \sum_{k=1}^{K-1} G_{m,z_k}(\tau_K - \tau_k) - \sum_{K=N_{i-1}+2}^{N_i} \sum_{k=1}^{K-1} G_{m,z_k}(\tau_{K-1} - \tau_k) \\ &= \sum_{K=N_{i-1}+2}^{N_i} \sum_{k=1}^{K-1} G_{m,z_k}(\tau_K - \tau_k) - \sum_{K=N_{i-1}+1}^{N_i-1} \sum_{k=1}^K G_{m,z_k}(\tau_K - \tau_k), \end{aligned}$$

where for the final equality we have simply relabelled the index  $K$  on the second summation term. To continue, we note that when the offspring density  $h_{\cdot,\cdot}(\cdot)$  is for a continuous random variable with non-negative support,

$G_{\cdot,\cdot}(\tau_K - \tau_K) = G(0) = 0$ . Therefore,

$$\begin{aligned} & \sum_{K=N_{i-1}+2}^{N_i} \sum_{k=1}^{K-1} G_{m,z_k}(\tau_K - \tau_k) - \sum_{K=N_{i-1}+1}^{N_i-1} \sum_{k=1}^K G_{m,z_k}(\tau_K - \tau_k) \\ &= \sum_{k=1}^{N_i-1} G_{m,z_k}(\tau_{N_i} - \tau_k) - \sum_{k=1}^{N_{i-1}} G_{m,z_k}(\tau_{N_{i-1}+1} - \tau_k). \end{aligned} \quad (6)$$

Combining (5) with (6) gives

$$\int_{t_{i-1}}^{\tau_{N_i}} \varphi_m(s) ds = \sum_{k=1}^{N_i-1} G_{m,z_k}(\tau_{N_i} - \tau_k) - \sum_{k=1}^{N_{i-1}} G_{m,z_k}(t_{i-1} - \tau_k). \quad (7)$$

Summing over  $m \in \mathcal{M}$  gives the desired result. Note that for the first observation time,  $t_1$ , the second summation in (7) is empty, yielding

$$\int_0^{\tau_{N_1}} \varphi_m(s) ds = \sum_{k=1}^{N_1-1} G_{m,z_k}(\tau_{N_1} - \tau_k).$$

## A.2 SMC with Exponential Kernel

For a MHP specified with exponential kernels, the intensity of type- $m$  events is given by

$$\lambda_m(t) = \nu_m(t) + \sum_{\tau_k < t} \frac{\eta_{m,z_k}}{\beta_{m,z_k}} \exp\left(-\frac{t - \tau_k}{\beta_{m,z_k}}\right).$$

Define the stochastic matrix  $\varepsilon(t) \in \mathbb{R}_+^{M \times M}$  to have entries

$$\begin{aligned} \varepsilon_{m,p}(t) &= \sum_{\tau_k < t} \frac{\eta_{m,z_k}}{\beta_{m,z_k}} \exp\left(-\frac{t - \tau_k}{\beta_{m,z_k}}\right) \mathbb{1}_{\{z_k=p\}} \\ &= \sum_{\tau_k < t} \frac{\eta_{m,p}}{\beta_{m,p}} \exp\left(-\frac{t - \tau_k}{\beta_{m,p}}\right) \mathbb{1}_{\{z_k=p\}}. \end{aligned}$$

Intuitively,  $\varepsilon_{m,p}(t)$  contains the contribution of type- $p$  events to the intensity  $\lambda_m$  to time  $t$ . Suppose that, on the  $i^{\text{th}}$  observation interval, events  $t_{i-1} <$

$\tau_{N_{i-1}+1} < \dots < \tau_{N_i} \leq t_i$  are observed. On  $(t_{i-1}, \tau_{N_{i-1}+1}]$ , we have

$$\begin{aligned}\varepsilon_{m,p}(t) &= \sum_{\tau_k < t} \frac{\eta_{m,p}}{\beta_{m,p}} \exp\left(-\frac{t_{i-1} - \tau_k}{\beta_{m,p}}\right) \mathbb{1}_{\{z_k=p\}} \cdot \exp\left(-\frac{t - t_{i-1}}{\beta_{m,p}}\right) \\ &= \varepsilon_{m,p}(t_{i-1}) \exp\left(-\frac{t - t_{i-1}}{\beta_{m,p}}\right).\end{aligned}$$

Letting  $K = N_{i-1} + 2, \dots, N_i$ , for  $t \in (\tau_{K-1}, \tau_K]$ , we get

$$\begin{aligned}\varepsilon_{m,p}(t) &= \sum_{\tau_k < t} \frac{\eta_{m,p}}{\beta_{m,p}} \exp\left(-\frac{\tau_{K-1} - \tau_k}{\beta_{m,p}}\right) \mathbb{1}_{\{z_k=p\}} \cdot \exp\left(-\frac{t - \tau_{K-1}}{\beta_{m,p}}\right) \\ &= \left( \varepsilon_{m,p}(\tau_{K-1}) + \frac{\eta_{m,p}}{\beta_{m,p}} \mathbb{1}_{\{z_{K-1}=p\}} \right) \cdot \exp\left(-\frac{t - \tau_{K-1}}{\beta_{m,p}}\right).\end{aligned}$$

The preceding expression shows that, for all  $m, p$ , the value  $\varepsilon_{m,p}(\tau_{K-1})$  is decayed on the increment  $(\tau_{K-1}, t]$ , but that the additional jump  $\eta_{m,p}/\beta_{m,p}$  must be included if the event at  $\tau_{K-1}$  is of type  $z_{K-1} = p$ . Finally, on  $(\tau_{N_i}, t_i]$ , we similarly have

$$\varepsilon_{m,p}(t) = \left( \varepsilon_{m,p}(\tau_{N_i}) + \frac{\eta_{m,p}}{\beta_{m,p}} \mathbb{1}_{\{z_{N_i}=p\}} \right) \cdot \exp\left(-\frac{t - \tau_{N_i}}{\beta_{m,p}}\right).$$

For completion, note that if no event is present on the  $(t_{i-1}, t_i]$ , then for  $t \in (t_{i-1}, t_i]$ ,

$$\varepsilon_{m,p}(t) = \varepsilon_{m,p}(t_{i-1}) \exp\left(-\frac{t - t_{i-1}}{\beta_{m,p}}\right).$$

With these values in hand, we can compute the integral present in the expression for  $\log w_i^{(j)}$ . Define  $\mathcal{E}(\cdot; \beta)$  to be the CDF of an exponential random variable with parameter  $\beta$ . Then

$$\int_{t_{i-1}}^{\tau_{N_{i-1}+1}} \varepsilon_{m,p}(t) dt = \varepsilon_{m,p}(t_{i-1}) \beta_{m,p} \mathcal{E}(\tau_{N_{i-1}+1} - t_{i-1}; \beta_{m,p}).$$

Again letting  $K = N_{i-1} + 2, \dots, N_i$ ,

$$\int_{\tau_{K-1}}^{\tau_K} \varepsilon_{m,p}(t) dt = \left( \varepsilon_{m,p}(\tau_{K-1}) + \frac{\eta_{m,p}}{\beta_{m,p}} \mathbb{1}_{\{z_{K-1}=p\}} \right) \beta_{m,p} \mathcal{E}(\tau_K - \tau_{K-1}; \beta_{m,p}).$$

To compute the desired integral, note that

$$\int_{t_i}^{\tau_{N_i}} \lambda(t) dt = \int_{t_i}^{\tau_{N_{i-1}+1}} \lambda(t) dt + \sum_{K=N_{i-1}+2}^{N_i} \int_{\tau_{K-1}}^{\tau_K} \lambda(t) dt. \quad (8)$$

Writing

$$\lambda(t) = \nu(t) + \sum_{m,p=1}^M \varepsilon_{m,p}(t),$$

the integrals in (8) are easily calculated by summing over the integrals previously derived. As before, we have

$$\int_{\tau_{N_i}}^{t_i} \varepsilon_{m,p}(t) dt = \left( \varepsilon_{m,p}(\tau_{N_i}) + \frac{\eta_{m,p}}{\beta_{m,p}} \mathbf{1}_{\{z_{N_i}=p\}} \right) \beta_{m,p} \mathcal{E}(t_i - \tau_{N_i}; \beta_{m,p}),$$

from which we calculate

$$\int_{\tau_{N_i}}^{t_i} \lambda(t) dt = \int_{\tau_{N_i}}^{t_i} \nu(t) dt + \sum_{m,p=1}^M \int_{\tau_{N_i}}^{t_i} \varepsilon_{m,p}(t) dt.$$

This expression is required for evaluating the approximation  $\hat{p}(\mathbf{n}_i \mid \mathbf{n}_{1:i-1})$ . Finally, consider the sum

$$\sum_{k=N_{i-1}+1}^{N_i} \log \lambda_{z_k}(\tau_k)$$

which is present in the expression for  $\log w_i^{(j)}$ . We have that

$$\lambda_{z_k}(\tau_k) = \nu_{z_k}(\tau_k) + \sum_{p=1}^M \varepsilon_{z_k,p}(\tau_k),$$

hence the sum in question can be incrementally computed via the matrix  $\varepsilon(t)$ . The advantage of the exponential case is that, through the representations provided, relevant values of the self-excitation effect  $\varepsilon(t)$  can be calculated recursively. This is of linear time complexity, and eliminates the need to store the complete history of a particle chain.

## B Simulation Experiments

Table 4 shows the results of the simulation experiment in the case where the matrix  $\beta$  is unconstrained<sup>3</sup>. The PMMH-MCMC estimates show similar performance to the MLE for aggregation levels of  $\Delta = 0.1, 0.5$ . The variability of the cross-excitation parameters  $\beta_{1,2}$  and  $\beta_{2,1}$  show greater variability than the two self-excitation parameters. Figure 8 displays the standard error of the PMMH-MCMC estimates compared to the censoring times  $T \in \{100, 200, 400\}$ . We see a linear trend with a gradient of approximately  $-0.5$ , which agrees with a convergence rate of  $\sqrt{T}$  to zero of the standard errors.

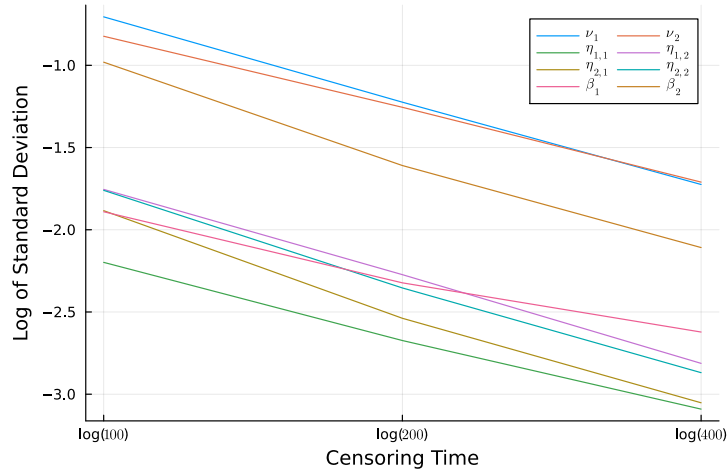


Figure 8: Standard deviation of estimates relative to time for PMMH-MCMC estimates.

---

<sup>3</sup>The values in Table 4 have been trimmed to remove extreme outliers. An outlier is defined as any value  $x$  satisfying  $x > Q3 + 5 \cdot IQR$  or  $x < Q1 - 5 \cdot IQR$ , where  $Q1$  and  $Q3$  are the 1<sup>st</sup> and 3<sup>rd</sup> quartiles of the particular sample, respectively, and  $IQR$  is the interquartile range. This typically removes fewer than 3% of the sample paths, though in extreme cases ( $\Delta = 5.0$ ) removes up to 8%

Table 4: Summary of results from PMMH-MCMC Simulation Experiment with general  $\beta$  structure,  $T = 200$ .

	$\nu_1$	$\nu_2$	$\eta_{1,1}$	$\eta_{1,2}$	$\eta_{2,1}$	$\eta_{2,2}$	$\beta_{1,1}$	$\beta_{1,2}$	$\beta_{2,1}$	$\beta_{2,2}$
True Params	0.8	1.0	0.6	0.3	0.25	0.5	0.5	0.5	0.75	0.75
$\Delta = 0$	Est	0.822	1.040	0.578	0.316	0.266	0.471	0.486	0.548	0.820
	SE	0.234	0.268	0.059	0.074	0.069	0.086	0.091	0.235	0.383
	$\widehat{SE}$	0.232	0.248	0.06	0.074	0.064	0.080	0.090	0.211	0.330
	CP	0.948	0.952	0.934	0.898	0.862	0.902	0.922	0.908	0.882
$\Delta = 0.1$	Est	0.792	1.018	0.587	0.308	0.258	0.481	0.495	0.568	0.813
	SE	0.263	0.290	0.060	0.083	0.078	0.091	0.090	0.258	0.379
	$\widehat{SE}$	0.242	0.259	0.061	0.078	0.067	0.083	0.094	0.279	0.378
	CP	0.946	0.944	0.946	0.948	0.934	0.932	0.958	0.918	0.906
$\Delta = 0.5$	Est	0.804	1.015	0.595	0.298	0.255	0.484	0.502	0.583	0.749
	SE	0.274	0.280	0.066	0.097	0.081	0.101	0.101	0.332	0.429
	$\widehat{SE}$	0.248	0.261	0.064	0.083	0.070	0.085	0.103	0.384	0.441
	CP	0.947	0.942	0.930	0.930	0.934	0.926	0.957	0.958	0.939
$\Delta = 1.0$	Est	0.831	1.001	0.604	0.279	0.260	0.483	0.515	0.577	0.681
	SE	0.331	0.302	0.080	0.126	0.095	0.109	0.120	0.434	0.467
	$\widehat{SE}$	0.258	0.263	0.068	0.089	0.072	0.088	0.119	0.502	0.480
	CP	0.930	0.930	0.922	0.898	0.902	0.910	0.944	0.959	0.939
$\Delta = 5.0$	Est	0.860	0.944	0.620	0.255	0.306	0.438	0.745	0.841	0.867
	SE	0.392	0.410	0.110	0.158	0.134	0.143	0.241	0.595	0.525
	$\widehat{SE}$	0.215	0.216	0.065	0.074	0.067	0.076	0.175	0.367	0.361
	CP	0.760	0.768	0.772	0.655	0.712	0.720	0.648	0.714	0.759

## C Applied Study

### C.1 Period of the US Exit

Figure 9 shows 500 sample paths simulated from the MCEM estimates of the terror attack data; the parameter estimates are significantly biased and do not agree with the observed counts. Figure 10 displays trace plots for the PMMH-MCMC estimation of the MHP model of terrorism in Afghanistan

and Pakistan during the US exit from Afghanistan. Good mixing is observed in the all chains other than  $\beta_2$ , driven the low values of  $\eta_{2,1}$  and  $\eta_{2,2}$ . Next, Figure 11 display normalised histograms of the PMMH-MCMC chains in Figure 10. The assumed normality of the distribution over the parameters is clearly satisfied, though the distributions of  $\eta_{1,2}$ ,  $\eta_{2,1}$  and  $\eta_{2,2}$  are truncated at zero. This suggests a lack of self-excitation in Pakistan and cross-excitation in the model.

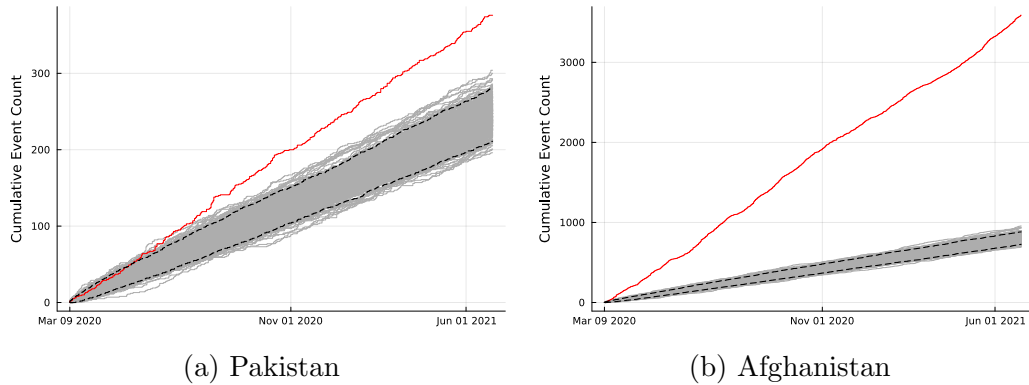


Figure 9: MCEM estimates of terrorism data during US Exit.

## C.2 2018 - 2021

Figure 12 shows trace plots for the PMMH-MCMC chain used to estimate the MHP model of terrorism in the extended period of 2018-2021, with Figure 13 displaying the corresponding histograms. We again observe good mixing of the chain, with clear improvement in the normality of  $\eta_{1,2}$  and  $\eta_{2,2}$ . We again note that low excitation in Pakistan makes  $\beta_2$  challenging to identify, hence the erratic trace plot and histogram.

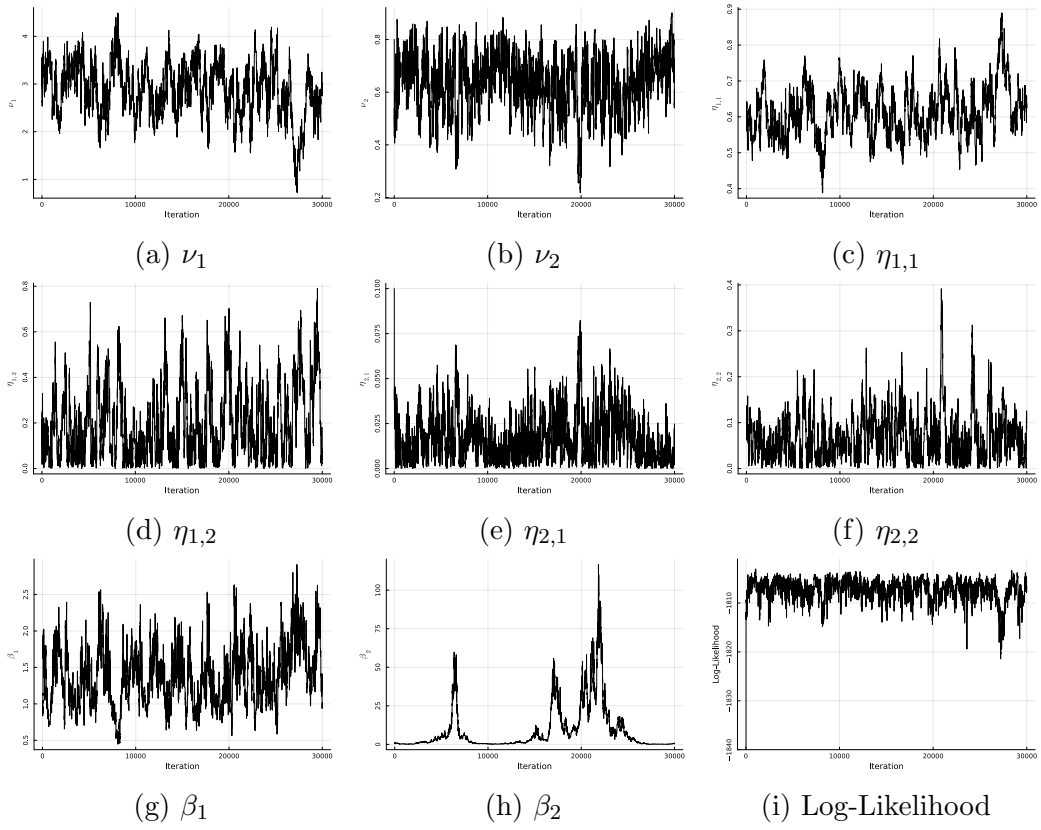


Figure 10: Trace plots for PMMH-MCMC estimation of terrorism in Pakistan and Afghanistan during the US Exit, presented in Section 4.1.

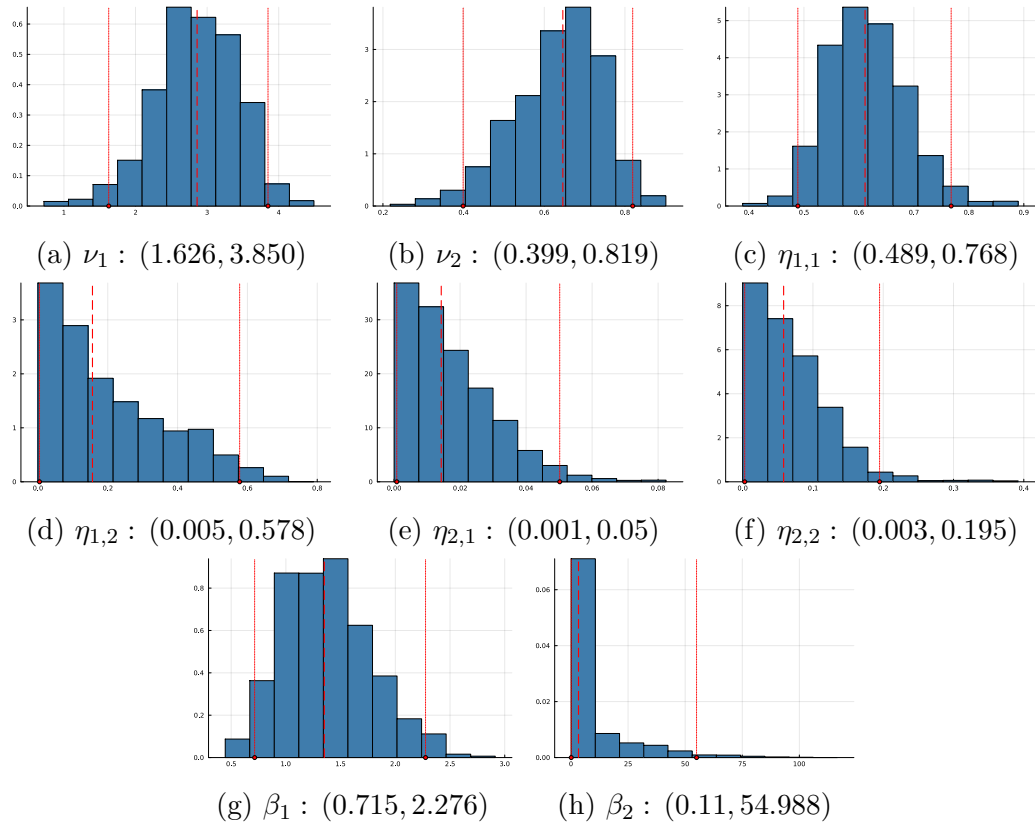


Figure 11: Histograms and 95% numerical confidence intervals for PMMH estimate of model in Section 4.1. Estimate (median) is marked in red dashed line, confidence interval with red dots on the horizontal axis.

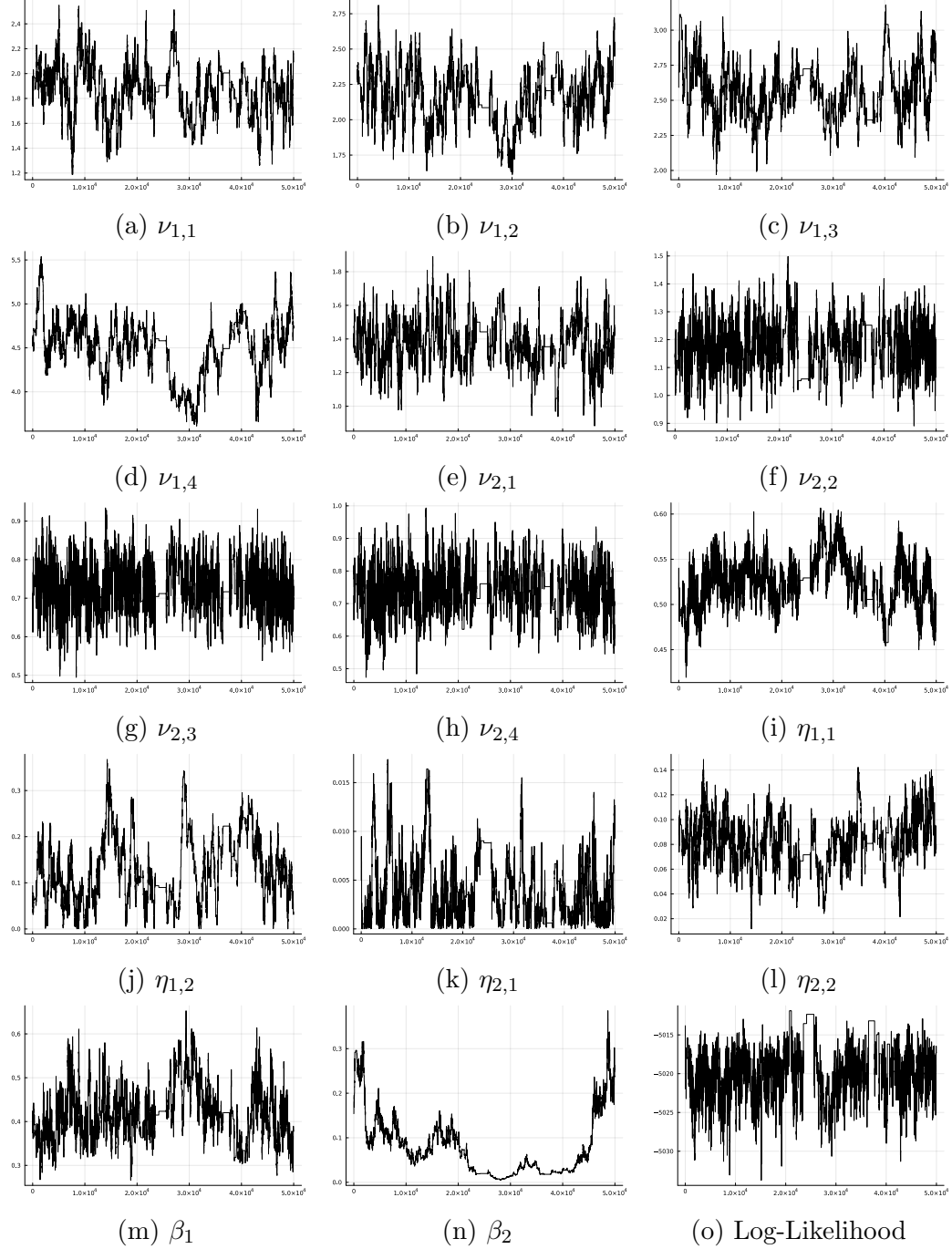


Figure 12: Trace plots for PMMH-MCMC estimation of terrorism in Pakistan and Afghanistan, 2018-2021, presented in Section 4.2.

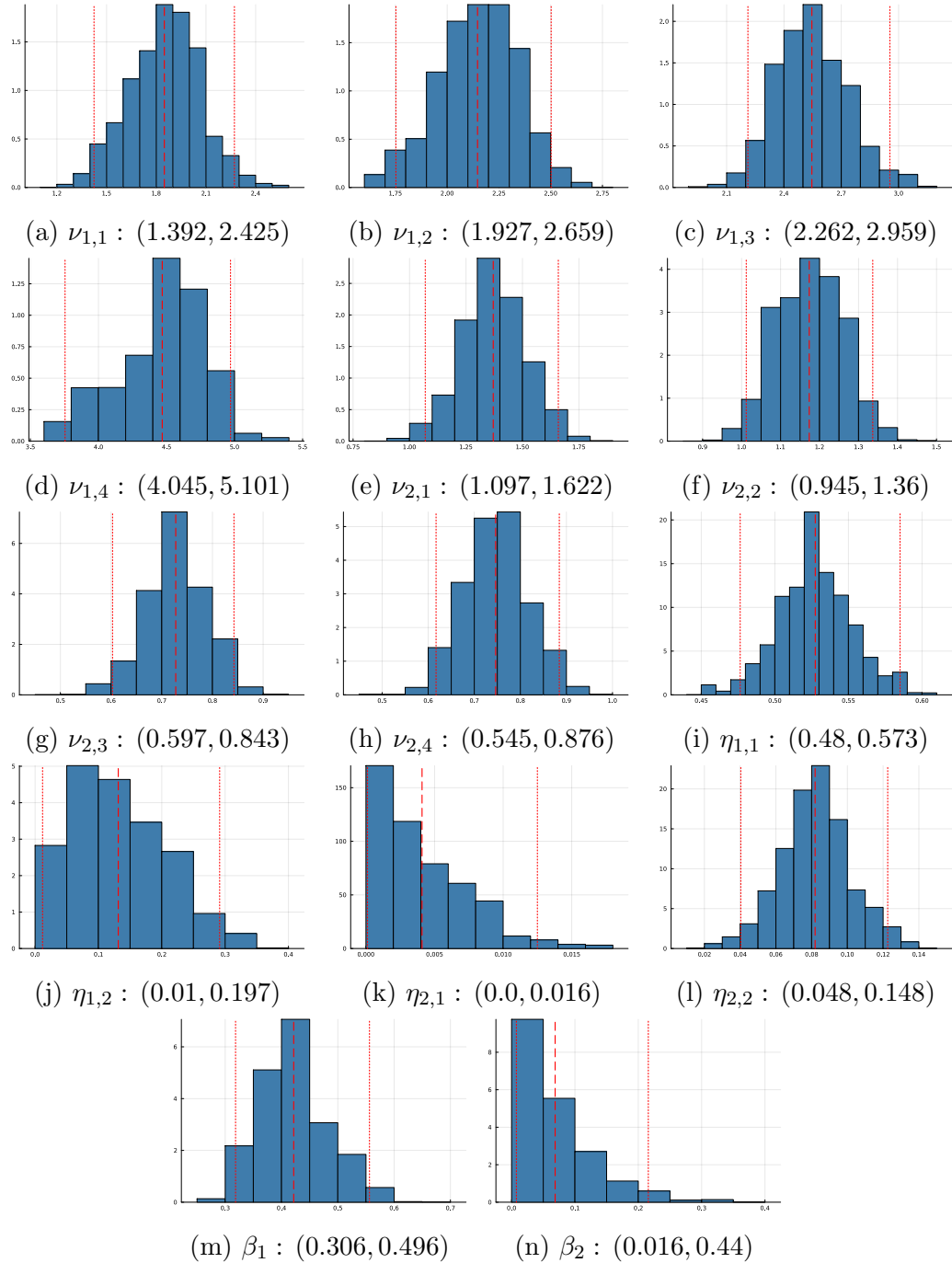


Figure 13: Histograms and 95% numerical confidence intervals for PMMH estimate of model in Section 4.2

## References

- Abbas, H. (2008). A Profile of Tehrik-i-Taliban Pakistan. *CTC Sentinel*, 1(2):1–5.
- Akhtar, S. and Ahmed, Z. S. (2023). Understanding the resurgence of the Tehrik-e-Taliban Pakistan. *Dynamics of Asymmetric Conflict*, 16(3):285–306.
- Andrieu, C., Doucet, A., and Holenstein, R. (2010). Particle Markov Chain Monte Carlo Methods. *Journal of the Royal Statistical Society Series B: Statistical Methodology*, 72(3):269–342.
- Andrieu, C. and Roberts, G. O. (2009). The pseudo-marginal approach for efficient Monte Carlo computations. *The Annals of Statistics*, 37(2).
- Aziz, S. (2023). Terrorism and tensions between Pakistan and Afghanistan: Are forced deportations the breaking point? <https://www.abc.net.au/religion/pakistan-and-afghanistan-forced-deportations-and-terrorism/103243728>. URL accessed 15/05/2024.
- Baldor, L. C. (2020). US begins troop withdrawal from Afghanistan, official says. <https://www.militarytimes.com/news/your-military/2020/03/09/us-begins-troop-withdrawal-from-afghanistan-official-says/>. URL accessed 15/05/2024.
- Behlendorf, B., LaFree, G., and Legault, R. (2012). Microcycles of Violence: Evidence from Terrorist Attacks by ETA and the FMLN. *Journal of Quantitative Criminology*, 28(1):49–75.
- Bonnet, A., Dion-Blanc, C., Gindraud, F., and Lemler, S. (2022). Neuronal network inference and membrane potential model using multivariate Hawkes processes. *Journal of Neuroscience Methods*, 372:109550.
- Bowsher, C. G. (2007). Modelling security market events in continuous time: Intensity based, multivariate point process models. *Journal of Econometrics*, 141(2):876–912.
- Calderon, P., Soen, A., and Rizoiu, M.-A. (2023). Linking Across Data Granularity: Fitting Multivariate Hawkes Processes to Partially Interval-Censored Data.

- Chen, B., Shrestha, P., Bertozzi, A. L., Mohler, G., and Schoenberg, F. (2022). A Novel Point Process Model for COVID-19: Multivariate Recursive Hawkes Process. In Bellomo, N. and Chaplain, M. A. J., editors, *Predicting Pandemics in a Globally Connected World, Volume 1*, pages 141–182. Springer International Publishing, Cham.
- Chen, F., Kwan, T.-K. J., and Stindl, T. (2025). Estimating the Hawkes process from a discretely observed sample path. *Journal of Computational and Graphical Statistics*, 0(ja):1–19.
- Cheysson, F. and Lang, G. (2022). Spectral estimation of Hawkes processes from count data. *The Annals of Statistics*, 50(3).
- Chopin, N. and Papaspiliopoulos, O. (2020). *An Introduction to Sequential Monte Carlo*. Springer Series in Statistics. Springer, Cham, Switzerland.
- Daley, D. J. and Vere-Jones, D. (2003). *An Introduction to the Theory of Point Processes*. Springer, New York, 2nd ed edition.
- Del Moral, P. (2013). *Mean Field Simulation for Monte Carlo Integration*. Number 126 in Monographs on Statistics and Applied Probability. CRC Press Taylor & Francis Group, Boca Raton London New York.
- Deligiannidis, G., Doucet, A., and Pitt, M. K. (2018). The Correlated Pseudomarginal Method. *Journal of the Royal Statistical Society Series B: Statistical Methodology*, 80(5):839–870.
- Devroye, L. (1986). *Non-Uniform Random Variate Generation*. Springer, New York Heidelberg.
- Doucet, A., Pitt, M. K., Deligiannidis, G., and Kohn, R. (2015). Efficient implementation of Markov chain Monte Carlo when using an unbiased likelihood estimator. *Biometrika*, 102(2):295–313.
- Doxsee, C., Thompson, J., and Hwang, G. (2021). Examining Extremism: Islamic State Khorasan Province (ISKP). <https://www.csis.org/blogs/examining-extremism/examining-extremism-islamic-state-khorasan-province-iskp>. URL accessed 15/05/2024.
- GTD (2022). Global Terrorism Database 1970 - 2021. *START (National Consortium for the Study of Terrorism and Responses to Terrorism)*.

- Hastings, W. K. (1970). Monte Carlo sampling methods using Markov chains and their applications. *Biometrika*, 57(1):97–109.
- Hawkes, A. G. (1971). Spectra of some self-exciting and mutually exciting point processes. *Biometrika*, 58(1):83–90.
- Hawkes, A. G. and Oakes, D. (1974). A cluster process representation of a self-exciting process. *Journal of Applied Probability*, 11(3):493–503.
- Hussain, A. (2023). What explains the dramatic rise in armed attacks in Pakistan? <https://www.aljazeera.com/news/2023/12/21/what-explains-the-dramatic-rise-in-armed-attacks-in-pakistan>. URL accessed 15/05/2024.
- Hussain, A. (2024). ‘Cousins at war’: Pakistan-Afghan ties strained after cross-border attacks. <https://www.aljazeera.com/news/2024/3/19/cousins-at-war-pakistan-afghan-ties-strained-after-cross-border-attacks>. URL accessed 15/05/2024.
- Jun, M. and Cook, S. (2024). Flexible multivariate spatiotemporal Hawkes process models of terrorism. *The Annals of Applied Statistics*, 18(2):1378–1403.
- Kirchner, M. (2017). An estimation procedure for the Hawkes process. *Quantitative Finance*, 17(4):571–595.
- Metropolis, N., Rosenbluth, A. W., Rosenbluth, M. N., Teller, A. H., and Teller, E. (1953). Equation of State Calculations by Fast Computing Machines. *The Journal of Chemical Physics*, 21(6):1087–1092.
- Middleton, L., Deligiannidis, G., Doucet, A., and Jacob, P. E. (2020). Unbiased Markov chain Monte Carlo for intractable target distributions. *Electronic Journal of Statistics*, 14(2).
- Midlarsky, M. I., Crenshaw, M., and Yoshida, F. (1980). Why Violence Spreads: The Contagion of International Terrorism. *International Studies Quarterly*, 24(2):262.
- Mullahy, J. (1986). Specification and testing of some modified count data models. *Journal of Econometrics*, 33(3):341–365.
- Oakes, D. (1975). The Markovian self-exciting process. *Journal of Applied Probability*, 12(1):69–77.

- Ogata, Y. (1978). The asymptotic behaviour of maximum likelihood estimators for stationary point processes. *Annals of the Institute of Statistical Mathematics*, 30(2):243–261.
- Perl, R. F. (2007). Combating Terrorism: The Challenge of Measuring Effectiveness. *Washington, DC: Congressional Research Services, Library of Congress*.
- Pitt, M. K. and Shephard, N. (1999). Filtering via Simulation: Auxiliary Particle Filters. *Journal of the American Statistical Association*, 94(446):590–599.
- Porter, M. D. and White, G. (2012). Self-exciting hurdle models for terrorist activity. *The Annals of Applied Statistics*, 6(1).
- Rieber-Mohn, J. H. and Tripathi, K. (2021). An investigation into microcycles of violence by the Taliban. *Security Journal*, 34(1):126–147.
- Rizoiu, M.-A., Soen, A., Li, S., Calderon, P., Dong, L. J., Menon, A. K., and Xie, L. (2022). Interval-censored hawkes processes. *Journal of Machine Learning Research*, 23(338):1–84.
- Sayed, A. and Hamming, T. (2023). The Tehrik-i-Taliban Pakistan After the Taliban’s Afghanistan Takeover. *Combating Terrorism Center at West Point*, 16(5):1–10.
- Schneider, P. J. and Weber, T. A. (2023). Estimation of self-exciting point processes from time-censored data. *Physical Review E*, 108(1):015303.
- Sherlock, C., Thiery, A. H., Roberts, G. O., and Rosenthal, J. S. (2015). On the efficiency of pseudo-marginal random walk Metropolis algorithms. *The Annals of Statistics*, 43(1).
- Shlomovich, L., Cohen, E. A. K., and Adams, N. (2022a). A parameter estimation method for multivariate binned Hawkes processes. *Statistics and Computing*, 32(6):98.
- Shlomovich, L., Cohen, E. A. K., Adams, N., and Patel, L. (2022b). Parameter Estimation of Binned Hawkes Processes. *Journal of Computational and Graphical Statistics*, 31(4):990–1000.

- Tench, S., Fry, H., and Gill, P. (2016). Spatio-temporal patterns of IED usage by the Provisional Irish Republican Army. *European Journal of Applied Mathematics*, 27(3):377–402.
- US Department of State (2024). Joint Statement of the U.S.-Pakistan Counterterrorism Dialogue. <https://www.state.gov/joint-statement-of-the-u-s-pakistan-counterterrorism-dialogue/>. URL accessed 15/05/2024.
- van der Vaart, A. W. (1998). *Asymptotic Statistics*. Cambridge Series in Statistical and Probabilistic Mathematics. Cambridge University Press, Cambridge, UK ; New York, NY, USA.
- Veen, A. and Schoenberg, F. P. (2008). Estimation of Space–Time Branching Process Models in Seismology Using an EM–Type Algorithm. *Journal of the American Statistical Association*, 103(482):614–624.
- White, G., Mazerolle, L., Porter, M., and Chalk, P. (2014). *Modelling the Effectiveness of Counter-Terrorism Interventions*. Australian Institute of Criminology.
- Yang, S. Y., Liu, A., Chen, J., and Hawkes, A. (2018). Applications of a multivariate Hawkes process to joint modeling of sentiment and market return events. *Quantitative Finance*, 18(2):295–310.
- Zammit-Mangion, A., Dewar, M., Kadirkamanathan, V., and Sanguinetti, G. (2012). Point process modelling of the Afghan War Diary. *Proceedings of the National Academy of Sciences*, 109(31):12414–12419.
- Zeidan, A. (2024). Withdrawal of United States troops from Afghanistan. <https://www.britannica.com/event/withdrawal-of-United-States-troops-from-Afghanistan>. URL accessed 15/05/2024.
- Zhou, L. and Papadogeorgou, G. (2023). Bayesian inference for aggregated Hawkes processes.